P517010.PDF [Page: 4 of 91]

Copy No. 31

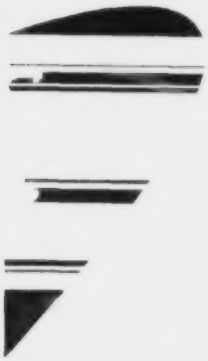

DEFENCE R&D DÉFENSE

Progressive Collapse Method for Ultimate Hull Girder Strength Assessment

M J Smith

Defence R&D Canada

Technical Memorandum
DREA TM 2001-145
October 2001

National Defence / Défense nationale

Canada

P517010.PDF [Page: 5 of 91]

104-06993/

Progressive Collapse Method for Ultimate Hull Girder Strength Assessment

M. J. Smith

Defence Research Establishment Atlantic

Technical Memorandum

DREA TM 2001-145

October 2001

Author

M. J. Smith

Approved by

J. L. Kennedy
Head/Warship Signatures and Safety

Approved for release by

K. Foster
Chair/Document Review Panel

© Her Majesty the Queen as represented by the Minister of National Defence, 2001

© Sa majesté la reine, représentée par le ministre de la Défense nationale, 2001

P51/010.PDF [Page: 7 of 91]

Abstract

This Memorandum provides a description of the theory and use of the progressive collapse method (PCM) for deterministic evaluation of ship hull girder ultimate strength. Bi-axial ultimate strength is considered, in which bending of a ship can occur about any axis in a cross-sectional plane perpendicular to the longitudinal axis. Two algorithms are examined for determining the ultimate strength: moment-curvature analysis, in which the curvature is incremented, and bi-axial strength analysis, in which the moment is incremented. The merits of these two algorithms are considered for determining interaction curves defining the envelope of bi-axial ultimate strengths. The load-carrying characteristics of individual structural units are also examined, and a review of the theory and assumptions is given. Two approaches for generating load-shortening response curves of longitudinally stiffened panels are considered in detail: one involves interpolation from precalculated load-shortening curves and the other involves the use of design equations. The implementation of the PCM in the RESULTS (RESidual and ULTimate Strength) programme is described, and a user's guide is provided. Validation of the code is performed using a steel box girder structure and two hypothetical damage case studies of the HALIFAX class warship.

Résumé

Ce mémoire décrit la théorie de la méthode de leffondrement en chaîne et son utilisation pour faire une évaluation déterministe de la résistance ultime des poutres de coque. Il examine le cas de la résistance ultime biaxiale où la courbure dun navire peut se produire autour de nimporte quel axe dans un plan de coupe transversale perpendiculaire à laxe longitudinal. Deux algorithmes de détermination de la résistance ultime sont examinés : lanalyse de la courbure en fonction du moment, avec incrémentation de la courbure. On étudie les mérites respectifs de ces deux algorithmes pour déterminer les courbes dinteraction qui définissent lenveloppe des résistances ultimes biaxiales. Les caractéristiques de la capacité portante déléments structuraux individuels sont aussi examinées, ainsi que la théorie et les hypothèses. On a examiné en détail deux méthodes de génération des courbes de réponse de panneaux raidis longitudinalement : lune par interpolation de courbes de raccourcissement des charges précalculées, lautre par des équations. On décrit lapplication de la méthode de leffondrement en chaîne dans le programme RESULTS (RESidual and ULTimate Strength) et on y donne un guide de lutilisateur. Pour la validation du code, on a utilisé une structure de poutre en caisson et deux études de cas de dommages hypothétiques dun navire de la classe HALIFAX.

THIS PAGE INTENTIONALLY LEFT BLANK

P517010.PDF [Page: 8 of 91]

Executive summary

Background

Ultimate hull girder strength analysis is used to determine the maximum bending loads that a ship hull can withstand. This is important not only at the design stage, but also throughout the life of the vessel as refits and changes in the weight distribution can affect both the strength and the loads on a ship. An ultimate strength programme ULTMAT was developed at DREA in the mid-1980s. Recently, the ULTMAT code has been completely re-developed based on the principles of the progressive collapse method (PCM). This method was developed in the 1970s to calculate the ultimate strength in first vertical, and then bi-axial bending of a hull. In addition to these efforts, DREA has recently led the development the Ultimate Strength Analysis Suite (ULTSAS), which provides a graphical interface for rapid, automatic generation of cross-sectional ultimate strength models from other ship structures applications.

Principal Results

The new ultimate strength analysis programme RESULTS (RESidual and ULTimate Strength) brings together in one application many of the concepts and advances that have been made in ultimate strength analysis over the last three decades. Validation results were obtained for a steel box girder structure, where the ultimate bending strength was found to be within 2% of experimental and finite element analysis results. Further validation was performed using two hypothetical damage case studies involving the HALIFAX class frigate. In these studies, RESULTS was found to give very similar results to the UK MOD ultimate strength programme NS94B.

Significance of Results

Ultimate hull girder strength is an important component of the ongoing ISSMM (Improved Ship Structure Maintenance Management) project. In fact, the requirement for a bi-axial capability in the ISSMM Software Tool (IST) was one of the principal reasons for the redevelopment of DREA's ultimate strength code. Plans have already been made to incorporate the RESULTS programme in the IST. The new code enables an envelope defining a ship's bi-axial strength limit to be calculated in about ten seconds using typical desktop hardware. This level of efficiency, when coupled with previous developments in ULTSAS for automated modelling, enables the code to be used effectively in design-level work as well as in damage assessments required for ISSMM.

P517010.PDF [Page: 9 of 91]

Future Work

The RESULTS programme is intended for use in ultimate and residual strength assessments of ships. This study has only dealt with the ultimate strength problem; the residual strength problem, which is important in multi-cyclic hull girder failure of vessels, is to be treated in an upcoming study. Another area of interest is in the quantification of the effects of the large number of uncertainties that arise in the ultimate strength analysis. For this, a probabilistic or reliability-based treatment is required, and the development of such an approach within the context of the RESULTS programme will be undertaken in the near future.

M. J. Smith; 2001; Progressive Collapse Method for Ultimate Hull Girder Strength Assessment; DREA TM 2001-145; Defence Research Establishment Atlantic.

P517010.PDF [Page: 10 of 91]

Sommaire

Généralités

On utilise lanalyse de la résistance ultime dune poutre de coque pour déterminer les charges maximales de courbure que peut supporter une coque. Cest important à létape de la conception, mais aussi pour toute la durée de vie du navire, car les travaux de remise à neuf et les changements dans la répartition des poids peuvent avoir une incidence sur la résistance et les charges exercées sur le navire. Au milieu des années 1980, le CRDA a développé le programme de résistance ultime ULTMAT. Récemment, le code ULTMAT a été refondu à partir des principes de la méthode de leffondrement en chaîne . Cette méthode a été mise au point dans les années 1970 pour calculer la résistance ultime dans la première verticale puis dans la courbure biaxiale de la coque. En plus de ces travaux, le CRDA a récemment dirigé le développement de ULTSAS (Ultimate Strength Analysis Suite) qui produit une interface graphique permettant la génération automatique rapide de modèles de résistance ultime de coupes transversales à partir dautres applications à des structures de navire.

Principaux résultats

Le nouveau programme danalyse de la résistance ultime RESULTS (RESidual and ULTimate Strength) regroupe en une application de nombreux concepts et les progrès qui ont été réalisés durant les trois dernières décennies dans le domaine de lanalyse de la résistance ultime. On a obtenu les résultats de validation pour une structure de poutre caisson en acier où on a constaté que la résistance ultime à la courbure concidait à 2 On a effectué une validation plus poussée avec deux études de cas de dommages hypothétiques sur la frégate de classe HALIFAX. Ces études ont permis de constater que RESULTS donnait des valeurs très proches du programme de résistance ultime UK MOD NS94B.

Importance des résultats

La résistance ultime des poutres de coque est une composante essentielle du projet ISSMM (Improved Ship Structure Maintenance Management) actuellement en cours. En fait, le besoin dune capacité biaxiale pour le logiciel ISSMM a été lune des principales raisons de la refonte du code de résistance ultime du CRDA. Il existe des plans pour incorporer le programme RESULTS au logiciel. Le nouveau code permet de calculer une enveloppe définissant la limite de résistance biaxiale du navire en environ dix secondes avec un ordinateur de bureau. En combinant ce niveau defficacité aux développements précédents dULTSAS pour la modélisation

P517010.PDF [Page: 11 of 91]

automatique, on peut utiliser efficacement le code à l'étape de la conception et pour les évaluations de dommages exigées pour ISSMM.

Futurs travaux

Le programme RESULTS sert à évaluer la résistance résiduelle et la résistance ultime des navires. Cette étude na abordé que la résistance ultime. Le problème de la résistance résiduelle, qui est important dans la défaillance multicyclique des poutres de coque, sera traité dans une étude ultérieure. Un autre point intéressant est la quantification des effets du grand nombre dincertitudes propres à lanalyse de résistance ultime. Pour cet aspect, un traitement probabiliste ou basé sur la fiabilité est nécessaire. Le développement de cette approche dans le contexte du programme RESULTS sera entrepris sous peu.

M. J. Smith; 2001; Progressive Collapse Method for Ultimate Hull Girder Strength Assessment; DREA TM 2001-145; Centre de Recherce pour la Défense Atlantique.

P517010.PDF [Page: 12 of 91]

Table of contents

Abstract i

Résumé i

Executive summary iii

Sommaire v

Table of contents vii

List of figures ix

1 Introduction 1

2 Background 2

3 Local Response Under Axial Loading 4

3.1 Structural Units 4

3.2 Qualitative Behaviour of Structural Units 5

3.2.1 Stiffened Panel Collapse Modes 6

3.2.2 Transversely Stiffened Panels 7

3.2.3 Corners 7

3.3 Stiffened Panel Parameters 8

3.4 Load-Shortening Curves 10

3.5 Effects of Weld-Induced Imperfections 12

3.6 Design Equations for Stiffened Panels 15

3.6.1 Gordo and Guedes Soares Equations 16

3.6.2 Rahman and Chowdhury Equations 16

3.6.3 Comparison with FE Curves 19

P517010.PDF [Page: 13 of 91]

4 Hull Girder Response and Ultimate Strength 20
4.1 Bi-Axial Moment-Curvature Analysis 20
4.2 Bi-Axial Static Strength 23
4.3 Interaction Curves 24
5 Implementation 26
5.1 Analysis Types 27
5.2 Cross Section Data Format 27
5.3 L-S Databases 28
6 Comparison with Test Results 28
6.1 Summary of Previous Test Measurements 28
6.2 Comparison with Akhras Box Girder 29
7 Application to Canadian Warships 34
7.1 Explosion Damage Case 34
7.2 Collision Damage Case 36
8 Conclusion 37
References 40
Annexes 44
A Load-Shortening Curve Data 44
B User's Guide to RESULTS 1.0 61
B.1 Master data file 61
B.1.1 Defining the analysis type 61
B.1.1.1 Bi-axial moment-curvature analysis 61
B.1.1.2 Hog and sag moment-curvature analysis . . . 62
B.1.1.3 Bi-axial static strength analysis 62

P517010.PDF [Page: 14 of 91]

B.1.1.4 Interaction curve analysis 62
B.1.1.5 First-yield bending moment analysis 63
B.1.1.6 Plastic bending moment analysis 63
B.1.2 Cross section data file 63
B.1.3 Materials data file 64
B.1.4 Load shortening curve databases 64
B.1.5 Results and other output files 65
B.2 Cross section data formats 65
B.2.1 ULTMAT format 65
B.2.2 Generic format 66
B.2.2.1 Longitudinally stiffened panels 67
B.2.2.2 Transversely stiffened panels 68
B.2.2.3 Hard corner units 68
B.3 Materials file format 68
B.4 Defining additional load shortening curves 69
B.5 Running RESULTS 69
List of symbols, abbreviations, acronyms and initialisms 70

List of figures

1 Three types of structural units used in the progressive collapse method. 5
2 A finite element model of a hard corner unit. 8
3 Hard corner load-shortening curves. 9
4 Finite element model of main deck stiffened panel. 11
5 Maximum distortion for an axially loaded panel 13

P517010.PDF [Page: 15 of 91]

6 Load-shortening curves of stiffened panels showing the effect of geometric distortion [33]. 14

7 Distribution of weld-induced axial stress in ship plating. 14

8 Load-shortening curves of stiffened panels showing the effect of residual stresses [33]. 15

9 Generic load-shortening curve [5]. 17

10 Warship cross-sectional model subdivided into structural units. 21

11 Cross section orientation showing the direction of curvature loading ϕ. 21

12 Algorithm for bi-axial moment-curvature analysis. 23

13 Algorithm for bi-axial static strength analysis. 24

14 Interaction curve obtained with bi-axial moment-curvature analysis. . . 25

15 Interaction curve obtained with bi-axial strength analysis. 26

16 Akhras box girder cross section [40]. 29

17 Box girder moment-curvature response in vertical bending predicted by RESULTS. 30

18 Box girder interaction curves predicted by RESULTS. 31

19 Finite element model of box girder under four-point bending. 32

20 Deformed shape of box girder structure in post-collapse region. 33

21 Deformed shape of box girder structure in post-collapse region (interior). 33

22 Vertical moment-curvature response of box girder structure. 34

23 HALIFAX class hull section, with damage region indicated. 35

24 Interaction curve for explosion damage test case. 36

25 Cross section with collision damage region indicated. 38

26 Interaction curve for collision deformation damage case. 39

P517010.PDF [Page: 16 of 91]

27 RESULTS interaction curves for two collision damage modelling approaches. 39

A.1 Curves for $\beta = 1$ and $\lambda = 0.3$. 45

A.2 Curves for $\beta = 1$ and $\lambda = 0.6$. 46

A.3 Curves for $\beta = 1$ and $\lambda = 0.9$. 47

A.4 Curves for $\beta = 1$ and $\lambda = 1.2$. 48

A.5 Curves for $\beta = 2$ and $\lambda = 0.3$. 49

A.6 Curves for $\beta = 2$ and $\lambda = 0.6$. 50

A.7 Curves for $\beta = 2$ and $\lambda = 0.9$. 51

A.8 Curves for $\beta = 2$ and $\lambda = 1.2$. 52

A.9 Curves for $\beta = 3$ and $\lambda = 0.3$. 53

A.10 Curves for $\beta = 3$ and $\lambda = 0.6$. 54

A.11 Curves for $\beta = 3$ and $\lambda = 0.9$. 55

A.12 Curves for $\beta = 3$ and $\lambda = 1.2$. 56

A.13 Curves for $\beta = 4$ and $\lambda = 0.3$. 57

A.14 Curves for $\beta = 4$ and $\lambda = 0.6$. 58

A.15 Curves for $\beta = 4$ and $\lambda = 0.9$. 59

A.16 Curves for $\beta = 4$ and $\lambda = 1.2$. 60

P517010.PDF [Page: 17 of 91]

1 Introduction

The ultimate hull girder strength of a ship defines the limiting bending load that the structure can withstand. Accurate knowledge of this is essential both at the design stage and throughout the life of the ship, and it is an important factor in determining a ship's weight limit and allowable operating conditions. Defence research organisations in various countries have developed computer codes for evaluating ultimate strength (ULTMAT in Canada [1], FABSTRAN/NS94 in the UK [2, 3, 4], and ULTSTR in the US [5]).

The progressive failure method (PCM) is a simplified two-dimensional modelling method that allows relatively fast and accurate calculation of ultimate strength. Rather than trying to model the true, three-dimensional behaviour of a ship, it instead assumes beam-like behaviour of the ship section under pure bending. PCM is applied to a ship cross section that has been subdivided into structural units according to the arrangement of longitudinal stiffeners, girders and plating.

The two programmes ULTMAT and FABSTRAN/NS94 have previously been used for hull girder ultimate strength calculations in DND. These two codes have recently been incorporated in the ULTSAS programme, which was developed by Martec Limited of Halifax, Nova Scotia under contract to DREA [6, 7, 8]. This programme provides a unified graphical user interface for the two codes and an automated cross-section generation capability which allows rapid ultimate strength assessments to be performed. Application of the ULTSAS software to warships was demonstrated in a recent study [9].

The ULTMAT code was first developed at DREA in the mid 1980s [1]. The original version of the code provided just the ultimate bending moment strengths in hog and sag. The approach made use of effective strength and limit state equations for stiffened panels and an equilibrium technique for finding the maximum bending moments. Later versions of the code adopted some of the concepts of the progressive collapse method first developed by Smith [10] for the NS94 codes, and were able to provide plots of the moment-curvature relationship in hog and sag. Still other versions of the code were created to calculate interaction curves describing a two-dimensional envelope of ultimate bi-axial bending moments at a given cross section.

Ultimate strength analysis is an essential component of the ongoing Improved Ship Structure Maintenance Management (ISSMM) Project [11]. This is a DRDC Major Project currently underway which aims to provide a software tool that will enable rapid risk assessments of CF vessels in a damaged condition. The first preference is to use an existing, Crown-owned programme such as ULTMAT, for the ultimate strength module of the ISSMM software tool (IST). Upon review of ULTMAT's

capabilities, it was determined that ULTMAT needed to have its bi-axial moment-curvature and interaction curve analysis capabilities upgraded for it to meet the requirements of the IST. A further reason to improve the code was based on a perceived need at DREA to extend its strength assessment capabilites to hull-girder residual strength assessments, where the remaining hull strength following a partial structural failure is determined. There is also interest in incorporating probabilistic and reliabililty methods in the strength assessment procedure to take account of uncertainities.

For these reasons the ULTMAT code has been completely redeveloped at DREA, and the new code will be known as RESULTS (Residual and Ultimate Strength). The new code has been designed to operate more or less seamlessly within the ULTSAS system, as it uses similar input formats for geometric definitions and load-shortening curve databases. This Memorandum gives a theoretical overview of the progressive failure method used by RESULTS to assess bi-axial ultimate strength. A description of the programme implementation is also provided. Numerical results are given for HALIFAX class damage case scenarios currently being developed for the purpose of validating the IST. A user's guide to the programme is provided in the annex.

2 Background

The term *ultimate strength* has been used to describe almost any failure mechanism involving buckling or collapse of the main hull girder or its components. In this study, ultimate strength refers to the maximum bending moment resistance of a ship hull girder structure. This strength will vary with the longitudinal position, but the amidships values are assumed to be the most significant because applied bending moments are greatest there. Strictly speaking, a hull-girder ultimate strength failure is a process that can occur over multiple load cycles and may involve dynamic effects such as whipping or slamming. But because of the considerable difficulties involved in treating the multi-cyclic problem, it is approximated as a quasi-static process in which the loading is applied monotonically. The treatment of ultimate strength assessment given in this study is deterministic, although it is understood that the large number of uncertainties that arise suggests the need for a probabilistic treatment as well.

The first approach to calculating ultimate strength that included both yield and collapse behaviour of the hull was provided by Caldwell [12]. He derived analytical equations for the strength of single-deck ships by lumping all of the structure into deck, bottom and side elements. The collapse behaviour was included in an averaged sense through the use of a strength reduction factor applied to the compressive elements. Although the approach is somewhat crude, strength predictions can

be obtained quickly making it useful for design-level calculations. Mansour and Thayambali [13] extended the Caldwell approach to consider lateral bending and twisting, as well as to consider the effects of combined bending moment loading and shear. Paik and Mansour [14] updated the Caldwell method by using more realistic distributions of the longitudinal stresses in the side elements.

A more complicated but more accurate approach to evaluating hull girder strength was developed by Smith [10], and will be referred to here as the progressive collapse method (PCM). The main features of this method are the division of a cross section into small, independently acting, structural units, the use of load-shortening curves to represent the compressive yielding/collapse behaviour of the structural units, and the use of an iterative numerical method to obtain the quasi-static bending response of the hull. In longitudinally stiffened warships, the majority of the structural units are stiffened panels, consisting of a single stiffener and its attached plating. The load-shortening characteristics of stiffened panels are similar to those of beam-columns, in which the attached plating forms a second flange.

This approach was introduced into the NS94 codes developed by the UK MOD [2, 3, 4]. In the earlier versions of the NS94 programmes (NS94A/B) the load-shortening characteristics were calculated by a separate programme (FABSTRAN) for each distinct stiffened panel unit. The FABSTRAN (Frame and Beam Static and Transient Response Analysis) programme used a non-linear finite element approach which included the non-linear geometric and material properties of the structure as well as lateral instability. Stiffened panels were modelled as beam-columns, with the web and flanges divided into a small number of thin 'fibres' used to help monitor the progress of material yielding. The later codes (NS94C/D) were supplied with a load-shortening curve database comprised of simple bi-linear curves calculated at regular intervals of plate and beam slenderness ratios. The load-shortening behaviour of a specific panel can then be interpolated from the curves in the database, without having to resort to additional finite element analyses.

The US Navy used a progressive collapse approach in its ULTSTR code in which the load carrying characteristics of stiffened panels were represented by design equations developed from known assumed states [5]. The limit states considered are two types of beam-column collapse (one where the direction of collapse is the same for adjacent bays, the other where the direction of collapse alternates) and tripping collapse of the stiffener. These, along with plastic hinge theory, were used to determine the ultimate strength of the structural units, as well as the pre- and post-collapse compressive response. The hull girder ultimate strength is determined by calculating the response to an applied curvature loading. Rahman and Chowdhury [15] used a similar approach to determine the vertical bending response of the hull girder. They modified Adamchak's design equations to conform with limit states for stiffened panels proposed by Hughes [16].

Gordo et al. [17, 18] used a similar progressive collapse approach, but they used different design equations for stiffened panel compressive response. These were obtained by combining equations for plating collapse with those of beam-column collapse [19]. Separate equations are derived assuming column buckling and tripping, and the one producing the smallest strength value for a given panel is used. A technique for incorporating residual stresses in the strength equations was also proposed. Hansen [20] also used a PCM-type approach in which the individual longitudinally stiffened panel units were assumed to respond like Euler beam-columns with constrained ends. In their analysis, the rotation angles at the ends of the beam-column are made compatible with the rotation of the section as a whole.

Finite element (FE) methods were originally used to determine hull-girder ultimate strength by Chen et al. [21]. This involves a finite element model of a section of a ship, and the application of forces or constraints to represent the bending moment load. Other three-dimensional FE studies were performed on a 1/3 scale model of a Leander class frigate [22]. The computational difficulties involved in such an approach are considerable, even with recent improvements in technology. Foremost among these is the way in which the bending load is applied. Displacement-controlled constraint loads, when used to rotate one end of a ship section, do not usually provide a pure bending load on a hull because they do not account for the shifting of the neutral axis position. A more effective approach is to use constraints distributed in the form of a four-point bending load, but this requires a larger, more expensive, model. On the other hand force-controlled loading does not work in the post-ultimate region, More advanced non-linear procedures, such as the arc-length method, generally perform poorly in complex structures where multiple instabilities can occur at once.

ISUM (Idealised Structural Unit Method) is a specialised finite element method that has been developed and applied to the problem of hull girder collapse, principally by Ueda and Rashed [23, 24]. They have developed a number of special purpose elements for plates, stiffened panels, and deep girders, which include geometric and material non-linear behaviour. The material non-linearities are handled using the plastic node method [25]. Bai et al. [26] developed an approach that is similar to ISUM.

3 Local Response Under Axial Loading

3.1 Structural Units

Figure 1 depicts the three types of structural units used to model a ship cross section. All the units are assumed to have lengths equal to the distance between transverse adjacent frames, but the frame spacing need not be the same for all units in the

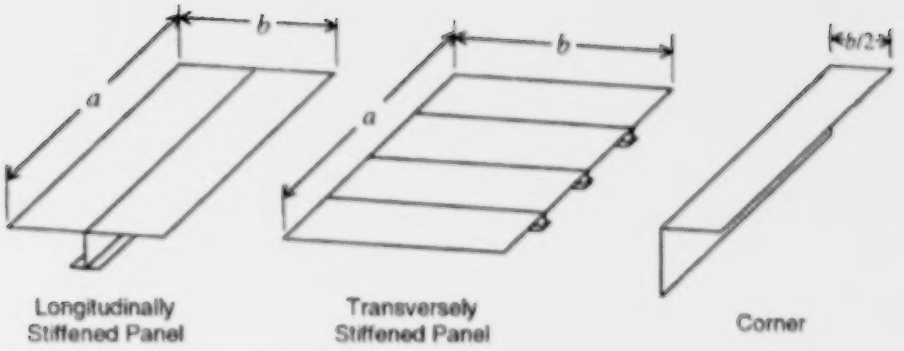

Figure 1: *Three types of structural units used in the progressive collapse method.*

section. The units do not include the frames, which are assumed to be rigid under longitudinal loading of the hull.

Longitudinally stiffened panel units are comprised of a single longitudinal stiffener and a quantity of attached plating. The amount of attached plating included in the structural unit is usually determined by dividing the plating equally among neighbouring stiffeners. Transversely stiffened panel units consist of sections of plating with transverse stiffeners. They may also be used to represent sections of unstiffened plating not included in any other longitudinal units. Corner units contain plating adjacent to the junctions of major structural components in the cross section, such as deck/side shell and deck/longitudinal bulkhead connections.

The three types of structural units can be used to represent most of the moment-resisting structure in a cross-section. Typically, the majority of structural units are longitudinally stiffened panels. Structure that is ineffective or partially effective in resisting moment loads, such as superstructure and other longitudinally discontinuous bulkheads and decks, may be omitted from the cross-sectional model.

One type of structure that is not well modelled by the three unit types are deep girders. Currently, they can be treated as assemblages of stiffened panels (transverse stiffened panels where tripping brackets are present) and hard corners. But a better approach may be to develop a special girder unit type with its own load carrying characteristics. This topic is left for a future investigation.

3.2 Qualitative Behaviour of Structural Units

In the PCM, the ultimate strength is determined from the load carrying characteristics of the individual structural units which comprise the hull girder structure at

a given cross section. The load carried by each structural unit under a statically applied sectional moment is determined by the local stress-strain characteristics of the independently acting unit. For units in compression these are given by so-called load-shortening (L-S) curves, which include lateral buckling instability effects as well as elastic and plastic compressive behaviour. For units in tension, load deflection curves are usually assumed to be linear elastic until yielding occurs, at which point the unit becomes perfectly plastic. This last assumption is appropriate for ship structural steels, which exhibit little strain hardening up to five or ten times the yield strain.

For the purpose of evaluating the ultimate strength, it is assumed that transverse frames are effectively rigid. This ignores the possibility of an overall grillage failure involving simultaneous collapse of the frames and longitudinal stiffeners. Fortunately this is an unlikely failure scenario and is relatively easy to design against [16]. Failure in compression is therefore assumed to occur as a result of some kind of inter-frame collapse of the stiffened panels. Typically this will be a chain reaction type failure in which one stiffened panel collapses, thus shedding load on to its neighbouring panels which in turn collapse, and so on. The post-collapse strength (residual strength) of individual units thus becomes important in determining the overall hull girder strength.

Structural units are assumed to act independently in resisting a bending moment load on the section; no iteraction between the structural units is permitted. This simplifying assumption is justified by the following reasoning. When a moment load is applied to a section, the resisting forces distribute themselves about the neutral axis, with compressive loads on one side and tension loads on the other. On the compression side, load shedding occurs in the plating between longitudinal stiffeners, causing the stiffeners to carry more and more of the unit's resisting load. Load shedding can continue to the point of collapse when the stiffened panels act essentially like independent beam-columns. On the tension side, the plating and stiffeners are constrained to maintain the original cross-sectional shape so that interaction among the tension-side units can be neglected.

3.2.1 Stiffened Panel Collapse Modes

Hughes [16] proposed three modes of collapse for longitudinally stiffened panels under combined compression and lateral loading as follows:

Mode 1: Collapse of the panel toward the plating (stiffener flange compression failure);

Mode 2: Collapse of the panel toward the stiffener (plating flange compression failure);

Mode 3: Combined failure of stiffener and plating (under large lateral loads).

Of these only the first two need to be considered here. The third mode occurs in conditions of large lateral loading and is therefore not relevant to the bending moment type hull failure considered in this study. The actual mode of failure is determined by whichever limit state (limiting stress value) is reached first under a given loading. This in turn depends on the dimensions, material properties, initial imperfections, and the magnitude and direction of any lateral loading that may be present.

In developing design equations for L-S curves, Adamchak [5] considered the following three modes of failure:

Mode 1: Panels in adjacent frames collapse in the same direction;

Mode 2: Panels in adjacent frames collapse in opposite directions;

Mode 3: Lateral-torsional failure of the stiffener (inelastic tripping).

Of these the third is the most difficult to predict, and is usually discounted through a conservative design with respect to elastic tripping. The first two modes differ primarily in the boundary conditions used where the stiffened panels join the frames.

3.2.2 Transversely Stiffened Panels

Transversely stiffened panels, which often occur in the side shell and longitudinal bulkhead structure, have two principal modes of behaviour in compression that depend on the aspect ratio of the grillage (the ratio of the stiffener spacing to the plate width) [3]. If the grillage ratio is less than one, both the plating and stiffeners deform laterally; for grillage ratios greater than or equal to one, only the plating deforms and the stiffeners are laterally rigid. In the latter case, the panel can be treated as unstiffened plating of appropriate aspect ratio.

3.2.3 Corners

Corner units are generally assumed to crush, rather than buckle, in compression, and are typically modelled assuming ideally elastic-plastic behaviour in which case they are called "hard corners". Figure 2 shows a corner unit in the HALIFAX class structure formed by the junction of the main deck and side shell. Non-linear finite element analysis of the unit produced a load-shortening curve shown in Figure 3, indicating that the corner does not reach its full plastic strength and hence that the

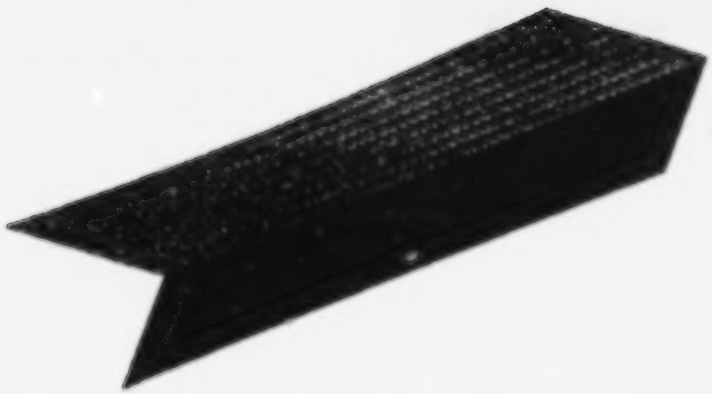

***Figure 2:** A finite element model of a hard corner unit.*

idealised elastic-plastic assumption is optimistic. The curve shown was obtained with 15 mm of lateral distortion in the deck and 6 mm of distortion in the side shell, which corresponds to a severe degree of plating imperfection, as will be discussed later in the chapter. The collapse of corner structures has not been extensively studied and warrants further investigation.

3.3 Stiffened Panel Parameters

To facilitate their use for a variety of materials and geometries, L-S curves for stiffened panels are recorded in terms of normalised stress and normalised strain quantities, i.e., the ratio of stress or strain to its yield value (see Figures 6 and 8). Longitudinally stiffened panels are characterised by three parameters: a plating slenderness ratio β, a column slenderness ratio λ, and an area ratio A_s/A. These ratios are determined by the panel dimensions and material properties as follows

$$\beta = b/t(\sigma_y/E)^{1/2} \qquad \lambda = (a/\pi r)(\sigma_y/E)^{1/2} \qquad A_s/A = A_s/(A_s + bt) \quad (1)$$

where b is the total width of the plating (Figure 1), t is the plating thickness, E is the elastic modulus, σ_y is the material yield stress, a is the overall length of the structural unit, and A_s is the cross-sectional area of the stiffener. The parameter r is the radius of gyration of the stiffener and its associated effective plating, and is determined by the formula

$$r = \sqrt{I_e'/A_e} \quad (2)$$

where $A_e = A_s + b_e t$ is the effective area of the stiffened panel cross section and I_e' is the effective second moment of area.

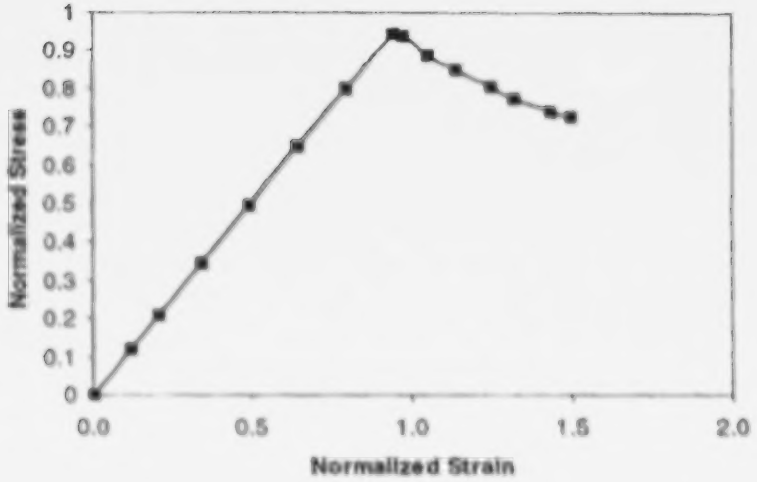

***Figure 3:** Hard corner load-shortening curves.*

The use of "effective" quantities to define the column slenderness is the result of nonuniform stress distributions that occur in plating between the stiffeners under compression. Considering a section of plating spanning two stiffeners, it is found that the average stress in the plating is generally less than the stress at the edge of the plating. This is due to the tendency of the plating to undergo a partial collapse at a load level considerably less than the ultimate strength of the beam-columns. This results in bulging of the plating and shedding of a portion of its load on to the neighbouring stiffeners. The effective width b_e of the plating is defined as the width that carries the same load at the edge stress value as the full width of plating carries at the lower, average stress value. This is expressed as

$$b_e \sigma_e = b \sigma_a \tag{3}$$

where σ_e and σ_a are the edge (maximum) and average stresses in the plating, respectively. Faulkner [27] proposed the following empirically derived formula for b_e, the effective width when yielding occurs at the plate edge ($\sigma_e = \sigma_y$)

$$\begin{aligned} b_e/b &= 2/\beta - 1/\beta^2 \qquad \beta > 1 \\ &= 1 \qquad\qquad\qquad\quad \beta \leq 1 \end{aligned} \tag{4}$$

where β is defined in Eqn. (1). The generalised form of b_e for intermediate stresses is obtained as

$$\begin{aligned} b_e/b = \sigma_a/\sigma_e &= 2/\beta_e - 1/\beta_e^2 \qquad \beta > 1 \\ &= 1 \qquad\qquad\qquad\quad \beta \leq 1 \end{aligned} \tag{5}$$

where

$$\beta_e = b/t\sqrt{\sigma_e/E} \tag{6}$$

The effective width b_e is used to define the axial load that can be carried by plating at a given stress level. Also of interest is the amount of additional load that can be carried at a given stress level. This is defined by a reduced effective width b'_e, which is obtained from

$$b'_e = b_e + \sigma_e \left(\frac{db_e}{d\sigma_e} \right) \tag{7}$$

Using (5), b'_e is obtained as

$$\begin{aligned} b'_e/b &= 1/\beta_e \qquad \beta > 1 \\ &= 1 \qquad \beta \leq 1 \end{aligned} \tag{8}$$

The reduced effective width is used to compute I'_e in the radius of gyration formula (2), used in the calculation of λ in Eqn. (1). It measures the resistance of the stiffened panel to collapse at a given load level, i.e. its ability to take on additional destabilizing load.

The column slenderness λ is related to the Euler elastic buckling load of a beam-column. If $\lambda = 1$, a stiffened panel will reach the critical load when the edge stress σ_e reaches yield. For $\lambda > 1$, the panel reaches the critical load before yielding, and therefore buckles elastically. For $\lambda < 1$, the panel yields before the critical load, and therefore buckles inelastically. Most stiffened panels in modern ship structures fall into the latter category.

3.4 Load-Shortening Curves

Considerable efforts have been made to characterize the load-shortening relationship of stiffened panels under static compression loads. L-S curves can be determined by design equations [5, 19, 15, 20], by testing [28], or by various nonlinear finite element techniques [10, 24, 26].

The latter approach was used to compile a database of L-S curves for longitudinally stiffened panels representative of those used in the HALIFAX class vessel [29, 30]. The curves were generated using plate/shell finite element models, like the one shown in Figure 4, and the VAST programme [31]. Two sets of models were used: an *end-to-end* set, in which the stiffened panels extend from one frame to another; and a *centre-to-centre* set in which the models span the mid-frame positions in two adjacent frames. The boundary conditions are slightly different for these two sets, and in general they produce different L-S curves.

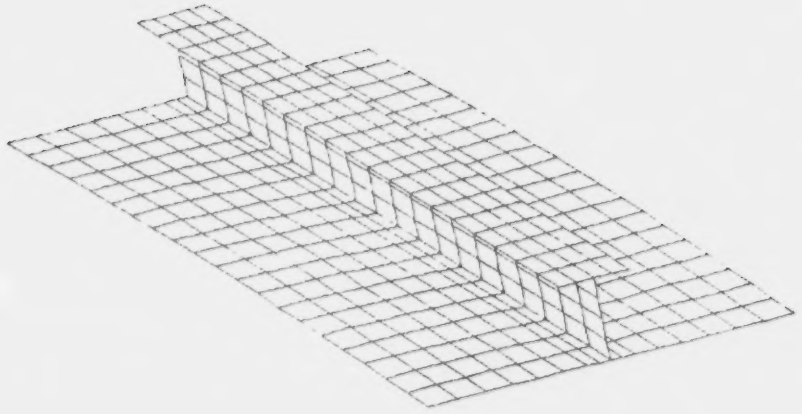

Figure 4: *Finite element model of main deck stiffened panel.*

Table 1: *Range of Parameters in the HALIFAX Class LSC Database*

Parameter	Values
Plate slenderness β	1, 2, 3, 4
Column slenderness λ	0.3, 0.6, 0.9, 1.2
Area ratio A_s/A	0.2, 0.275, 0.35
Maximum plate imperfection $\delta_p/\beta^2 t$	0.1, 0.2, 0.3
Maximum stiffener imperfection δ_s/a	0.001
Plating residual stress ratio σ_r/σ_y	0.15

Table 1 lists the range of parameters for which L-S curves were generated in the HALIFAX class database. The L-S curve to be used for any given stiffened panel can be linearly interpolated from the database curves for intermediate values β, λ, and A_s/A. In cases where the parameters of a stiffened panel fall outside those in the database, the L-S behaviour has to be extrapolated from the database curves. Unfortunately, the values of λ were determined using the full width rather than the effective width of plating [29]. Small errors can be expected in the L-S curves as a result of this oversight.

Another approach is to use bi-linear approximations of the true L-S curves so as to allow rapid assessment of ultimate hull strength, as has been done in the NS94C/D codes [3, 32]. Table 2 gives the range of parameters represented in the NS94 database for longitudinally stiffened panels.

The NS94C/D database also contains L-S curves for transversely stiffened panels. This type of unit is characterised by an aspect ratio $\alpha = a/b$ and the plating slender-

P517010.PDF [Page: 28 of 91]

Table 2: *Range of Parameters in the NS94 Longitudinally Stiffened LSC Database*

Parameter	Values
Plate slenderness β	1, 2, 3, 4
Column slenderness λ	0.2, 0.4, 0.6, 0.8, 1.0
Area ratio A_s/A	0.2
Maximum plate imperfection $\delta_p/\beta^2 t$	0.1

Table 3: *Parameters Represented in the NS94 Transversely Stiffened LSC Database*

Parameter	Values
Plate slenderness β	1, 1.5, 2, 3, 4
Aspect ratio α	1.0, ∞
Maximum plate imperfection $\delta_p/\beta^2 t$	0.1

ness β. The NS94C/D database provides curves for panels with parameters given in Table 3. For values of α in the range $1 \leq \alpha < \infty$, nonlinear interpolation is used according to an empirically derived formula reported by Dow [3]:

$$K = e^{-0.693\sqrt{\alpha - 1}} \tag{9}$$

where K and $1-K$ are the weightings of curves for $\alpha = 1$ and $\alpha = \infty$, respectively. The database curves do not apply for aspect ratios in the range $\alpha < 1$. Intermediate values of β are interpolated linearly, as is done for longitudinally stiffened panels.

3.5 Effects of Weld-Induced Imperfections

Welding of ship structure introduces geometric distortions and residual stresses, both of which have the effect of reducing compressive strength. Geometric distortions occur in both the plating and the stiffeners. Under a compressive loading force P, a panel with a maximum out-of-plane distortion of δ will experience a destabilising moment of $P\delta$ at the point of maximum distortion (Figure 5). Therefore knowing the maximum distortion alone gives an understanding of the degree of weakening, even if the exact shape of the distortion throughout the panel is not known. Based on this observation, the distortion can be effectively modelled by any convenient assumed shape with an amplitude equal to the maximum distortion.

The maximum distortion in the plating and stiffener can be denoted as δ_p and δ_s, respectively. For the purposes of this study, the stiffener distortion is represented as a half-sine wave of amplitude δ_s. The plating distortion is represented as a double

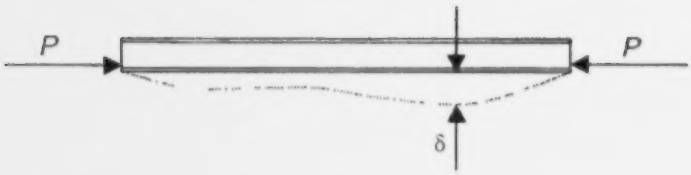

Figure 5: *Maximum distortion for an axially loaded panel*

Table 4: *Plating Distortions and Residual Stress Levels [32]*

Level	Plating Distortion δ_p	Residual Stress σ_r/σ_y
Slight	$0.025\beta^2 t$	0.05
Average	$0.1\beta^2 t$	0.15
Severe	$0.3\beta^2 t$	0.3

half-sine of amplitude δ_p and is superimposed on the stiffener distortion, so that the maximum total distortion in the plating is $\delta_p + \delta_s$, provided δ_p and δ_s are positive in the same direction.

Smith et al. [32] quantified plating distortions as multiples of $\beta^2 t$. They defined three levels of plating distortions, "slight", "average" and "severe", based on the 3-percentile, mean and 97-percentile values of δ_p determined from surveys of ship plating. The numerical values for these levels are given in Table 4. Somewhat different values were used in the three levels of plating imperfection used in the HALIFAX class database, given in Table 1.

Stiffener distortions can be more important as a strength reduction factor than plating distortions. Figure 6 shows that the effect of different values of d is to alter the ultimate strength of the panel, without significant impact on the pre- and post-ultimate behaviour. Stiffener distortions of $\delta_s = a/750$ or less are considered acceptable for warship construction [15]. Values of $\delta_s = a/1000$ were used in the HALIFAX class database.

Residual stresses are typically modelled by assuming that as a result of welding a a block of material of width ηt on either side of the weld has yielded in tension [27]. Figure 7 shows this for the weld between the web and the plating. A residual stress is then formed in the remainder of the plating to balance the tension blocks. Assuming this residual stress is uniform, it is obtained as:

$$\frac{\sigma_r}{\sigma_y} = \frac{2\eta}{b/t - 2\eta} \tag{10}$$

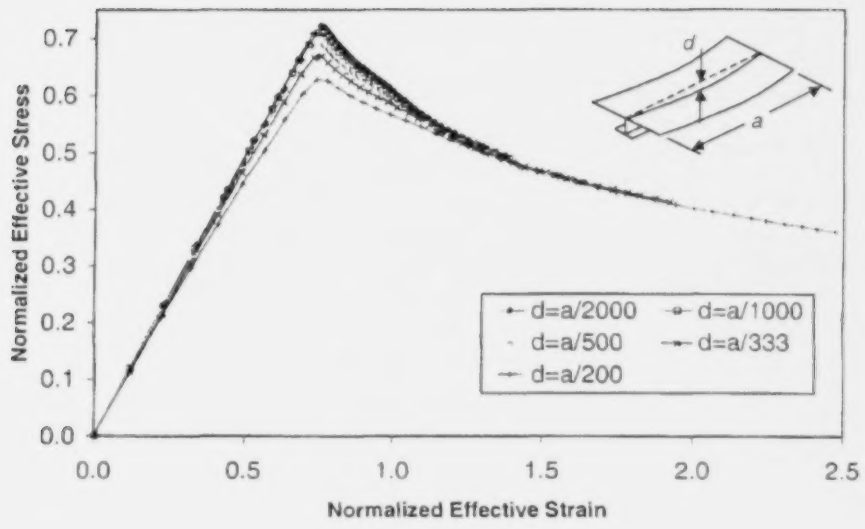

Figure 6: *Load-shortening curves of stiffened panels showing the effect of geometric distortion [33].*

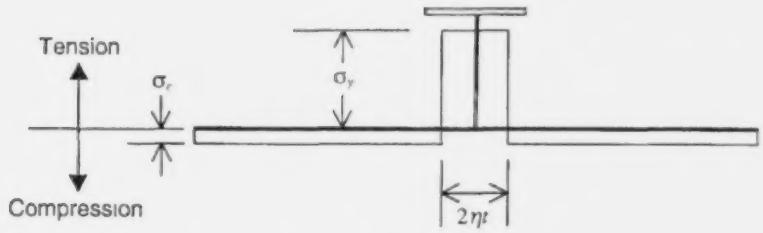

Figure 7: *Distribution of weld-induced axial stress in ship plating.*

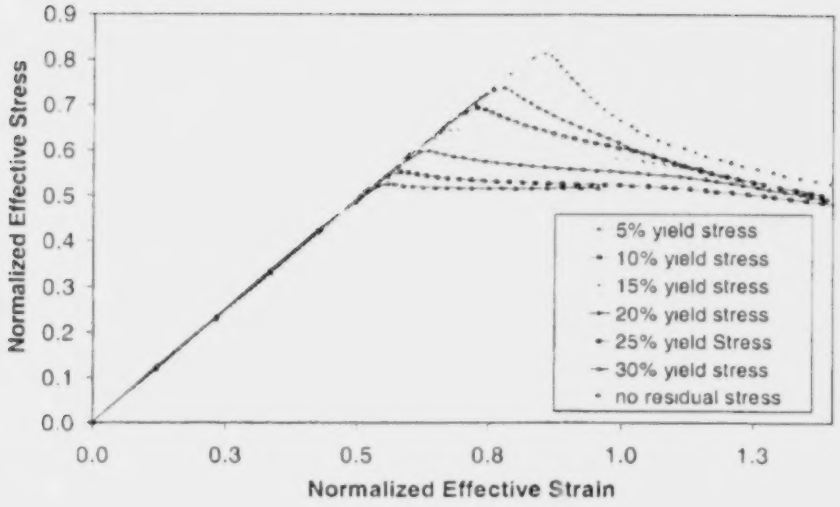

Figure 8: *Load-shortening curves of stiffened panels showing the effect of residual stresses [33].*

L-S curves of a stiffener panel with different amounts of residual stress are shown in Figure 8. The effect of increasing residual stress is both to reduce the ultimate strength and to lower the strain at which the ultimate strength occurs. Residual stresses also have a significant impact on the post-collapse behaviour.

3.6 Design Equations for Stiffened Panels

An alternative to using a predetermined database of L-S curves is to calculate directly the load-carrying capacity at a given strain level with design equations. This approach was used in the US Navy ultimate strength code [5], and has since been used by a number of others [19, 15, 20]. The advantage of using design equations is that calculation can be carried out quickly and can be done without interpolating from a large amount of stored data. The inclusion of design equations in the RESULTS ultimate strength programme would also assist future developments in residual and probabilistic strength assessment. The disadvantage is that design equations are necessarily approximations of the real response, and tend to be conservative, as is required for design-level work. Two different sets of design equations are presented here as candidates for inclusion in the RESULTS code. Both geometric distortions and residual stresses can to some extent be included in the design equations. Their accuracy is assessed by comparison with FE-generated curves in the HALIFAX class database.

P517010.PDF [Page: 32 of 91]

3.6.1 Gordo and Guedes Soares Equations

Gordo and Guedes Soares [19] assumed that a stiffened panel would collapse laterally toward the stiffener, and ignored the possibility of stiffener tripping. They proposed that the normalised average axial stress ($\overline{\sigma}_a = \sigma_a/\sigma_y$) in the panel as a function of normalised strain ($\overline{\epsilon} = \epsilon/\epsilon_y$) is given by

$$\overline{\sigma}_a = \Phi_{jo}(\overline{\epsilon})\frac{A_s + b_e(\overline{\epsilon})t}{A_s + bt} \tag{11}$$

where $b_e(\overline{\epsilon})$ is the instantaneous effective width of the plate flange. $\Phi_{jo}(\overline{\epsilon})$ is a strength parameter given by the Johnson-Ostenfeld formula for inelastic column buckling

$$\begin{aligned} \Phi_{jo}(\overline{\epsilon}) &= (1 - 1/4\Phi_E(\overline{\epsilon}))\,\Phi_e(\overline{\epsilon}), && \Phi_E(\overline{\epsilon}) > 0.5 \\ &= \Phi_E(\overline{\epsilon})\Phi_e, && \Phi_E(\overline{\epsilon}) \le 0.5 \end{aligned} \tag{12}$$

where

$$\Phi_E(\overline{\epsilon}) = 1/\lambda^2\overline{\epsilon} \tag{13}$$

and

$$\begin{aligned} \Phi_e(\overline{\epsilon}) &= -1, && \overline{\epsilon} < -1 \\ &= \overline{\epsilon}, && -1 < \overline{\epsilon} < 1 \\ &= 1, && \overline{\epsilon} > 1 \end{aligned} \tag{14}$$

In these expressions, compressive strain and stress are assumed to be positive.

Residual stresses in the plating are accounted for by replacing the effective width b_e with

$$b_{er} = b_e(\overline{\epsilon})\Phi_R(\overline{\epsilon}) \tag{15}$$

where

$$\Phi_R(\overline{\epsilon}) = \min\left(\Phi_e(\overline{\epsilon}), \Phi_r(\overline{\epsilon})\right)/\overline{\epsilon}, \qquad \Phi_r(\overline{\epsilon}) = \frac{\overline{\sigma}_r\overline{\epsilon} + 1 - \overline{\sigma}_r}{1 + \overline{\sigma}_r} \tag{16}$$

3.6.2 Rahman and Chowdhury Equations

Rahman and Chowdhury [15] combined the limit states developed by Hughes [16] and the plastic hinge approach used by Adamchak [5] to develop L-S curves for stiffened panels in one of two possible lateral collapse modes (Modes 1 and 2 proposed by Hughes). They also ignored stiffener tripping as a possible collapse mode.

Figure 9 shows a general form of the L-S curve developed by Adamchak. The curve has three zones: a stable zone, a no load-shedding zone and a load-shedding zone. According to the method developed by Adamchak, the stable zone is linear and extends up to the onset of yielding in the compressed panel. At that point the

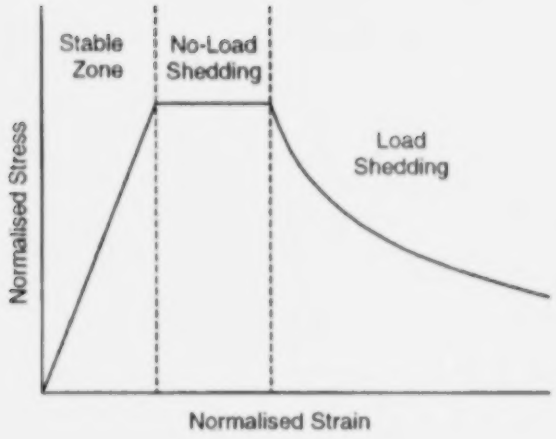

Figure 9: *Generic load-shortening curve [5].*

stiffened panel has reached its ultimate strength. As strain is increased further the average stress remains at that level until a plastic hinge has fully developed, marking the extent of the no load-shedding zone. Once the plastic hinge development is complete, the panel enters the load-shedding zone where the load carried by the panel must decrease in order to shorten the panel. As the panel is compressed further, it deforms like two rigid links rotating about the hinge. The extreme ends of the panel are assumed to be simply supported, and so no additional hinges are needed to complete the mechanism.

Rahman and Chowdhury [15] used the same approach but used limit states developed by Hughes (Modes 1 and 2, see Section 3.2.1) to define the onset of the no load-shedding zone. The equations for these limit states are too complicated to be reproduced here but can be found in Reference [16]. It is sufficient to state that the ultimate strength of the panel (i.e., the stress level in the no load-shedding zone) is given by

$$\overline{\sigma}_{ult} = \min(\overline{\sigma}_{uf}, \overline{\sigma}_{up}) \tag{17}$$

where $\overline{\sigma}_{uf}$ is the ultimate strength assuming the stiffener flange yields first (Mode 1), and $\overline{\sigma}_{up}$ is the ultimate strength assuming the plate flange yields first (Mode 2). They also modified the stable zone to account for inelasticity in the plating that occurs in a Mode 2 collapse. They did this by defining the axial response in the stable zone as

$$\begin{aligned} \sigma &= E\epsilon && \text{Mode 1} \\ &= (A_r/A)E\epsilon && \text{Mode 2} \end{aligned} \tag{18}$$

The quantity A_r is a reduced cross-sectional area that takes into account the plate

flange inelasticity, and is given by

$$A_r = A_s + bT_r \tag{19}$$

where

$$\begin{aligned} T_r &= 1 && \epsilon \leq \epsilon_{ult}/2 \\ &= 1 + \frac{T-1}{\epsilon_{ult}/2}(\epsilon - \epsilon_{ult}/2) && \epsilon_{ult}/2 < \epsilon \leq \epsilon_{ult} \end{aligned} \tag{20}$$

In these expressions, ϵ_{ult} is the strain at the onset of the no load-shedding zone, given by

$$\begin{aligned} \epsilon_{ult} &= \sigma_{ult}/E && \text{Mode 1} \\ &= \frac{A}{A_s + b_e t} E\epsilon && \text{Mode 2} \end{aligned} \tag{21}$$

The parameter T is a reduction factor defined with the secant modulus, as follows

$$T = \frac{E_s}{E} = 0.25\left(2 + \xi - \sqrt{\xi^2 - 10.4/\beta^2}\right) \tag{22}$$

where $\xi = 1 + 2.75/\beta^2$.

The plastic hinge is assumed to develop at the mid-point of the panel where the elastic bending moment is largest. If M_p is the plastic moment of the panel cross section, the maximum lateral deflection at the end of the no load-shedding zone is given by

$$w_{max} = \frac{M_p - qa^2/8}{P_{ult}} - w_{ult} \tag{23}$$

where q is the lateral load per unit length on the panel, P_{ult} is the ultimate axial load carried by the panel throughout the no load-shedding zone, and w_{ult} is the maximum lateral deflection at the beginning of the no load-shedding phase. Knowing this, the strain at the end of the no load-shedding zone ϵ_{pl} can be determined to be

$$\epsilon_{pl} = \epsilon_{ult} + \frac{1}{4}\left(\frac{\pi w_{max}}{a}\right)^2 \tag{24}$$

where ϵ_{ult} defines the strain at the beginning of the no load-shedding zone.

From the kinematics of the mechanism, the maximum lateral deflection in the load shedding zone can be determined as a function of strain to be

$$w_T = \left((w_{ult} + w_{max})^2 + \frac{a^2}{4}\left[(1 - \epsilon_{pl})^2 - (1 - \epsilon)^2\right]\right)^{1/2} \tag{25}$$

in which $\epsilon > \epsilon_{pl}$ represents the instantaneous axial strain. The axial stress can then be calculated from the formula

$$\sigma = \frac{M_p - qa^2/8}{(A_s + b_e t)w_T} \tag{26}$$

P517010.PDF [Page: 35 of 91]

3.6.3 Comparison with FE Curves

L-S curves obtained with the design curves are compared with the HALIFAX class database curves in Annex A.

Both of the design equations match well with the FE curves in the stable zone, with the exception of the Rahman equations for very slender plates ($\beta = 4$). The Gordo equations give the best estimate of the ultimate strength, compared with the FE curves, for stocky plates ($\beta = 1$), but overestimates the ultimate strength for the most slender plate and column combinations ($\beta \geq 3$, $\lambda \geq 0.9$). On the other hand, the flat response in the no-load shedding zone predicted with the Rahman equations tends to be conservative. In the post-collapse region the Gordo equations match with the FE curves best for stocky columns ($\lambda \leq 0.6$), while the Rahman equations seem to match best for the most slender columns ($\lambda \geq 0.9$). This suggests that the Gordo equations may be better suited for predicting inelastic collapse, whereas the Rahman equations may be better for predicting elastic or near-elastic buckling. In general, both design equations tend to overestimate the post-buckling stress levels. Overall the Rahman equations are more conservative, especially near the ultimate value, and may be safer to use. But neither of the design equations give entirely satisfactory predictions of the FE curves.

The two sets of FE curves (end-to-end and centre-to-centre) show significant discrepancies in the collapse and post-collapse region. These discrepancies can be attributed to the differences in the restraints in the two types of models. The end-to-end models use simply-supported conditions to model the influence of the frames, and do not account for the continuation of the stiffener to the next bay. The centre-to-centre models use symmetry conditions at the centre positions and a simply-supported constraint to model the influence of the frame. The significant difference is that the centre-to-centre models incorporate the continuation of the stiffener through the frame, and therefore provide a more realistic restraint effect at a frame. The torsional resistance of a frame itself is ignored as negligible in both types of models.

The assumptions used in the Rahman equations are more similar to those of the centre-to-centre FE models, whereas the assumptions used in the Gordo equations are more similar to the end-to-end FE models. But these similarities are not apparent in the plots in Annex A.

P517010.PDF [Page: 36 of 91]

4 Hull Girder Response and Ultimate Strength

In the Progressive Collapse Method (PCM), it is assumed that the two-dimensional plane of the section remains plane under moment loading. Thus, knowing the bi-axial curvature at the section, it is possible to determine the strain in the individual structural units. Static loads are applied incrementally, starting at zero, and increase until hull girder failure occurs and beyond. Static loads can be applied as increments of curvature or moment, depending on the type of ultimate strength assessment that is performed. Moment-curvature analysis uses increments of curvature as the load, and in this case the section can be loaded well beyond the collapse load. For bi-axial strength and interaction curve analysis, on the other hand, it is best to use increments of bending moment as the loading, in which case the increments stop when the maximum moment is achieved.

Figure 10 shows a typical cross section of a warship with the different types of structural units indicated.

4.1 Bi-Axial Moment-Curvature Analysis

In bi-axial moment-curvature analysis, a hull's resisting bending moment is determined as a function of the curvature of its beam-like deflected shape, measured at a particular cross-section of the hull. The analysis is carried out by repeatedly incrementing the curvature, and at each step calculating the net moment due to the forces induced in the structural units. The force in each unit is determined from its assumed or computed load-deflection characteristics, and by the local unit strain. The latter is obtained directly from the curvature, assuming that the plane of the section remains plane under deformation.

Bending moment and curvature are vector quantities with components in the horizontal and vertical directions. They are referenced to axes passing through the instantanteous centroid of the section. The curvature is incremented in a fixed direction ϕ measured from the horizontal axis, as shown in Figure 11. Thus, the curvature vector can be expressed as

$$\kappa = \{\kappa_h \; \kappa_v\} = \|\kappa\|\{\sin\phi \; \cos\phi\} \tag{27}$$

As the curvature is incremented, the moment vector is determined from the equation of beam flexure

$$\begin{Bmatrix} M_h \\ M_v \end{Bmatrix} = \begin{bmatrix} D_{hh} & D_{hv} \\ D_{hv} & D_{vv} \end{bmatrix} \begin{Bmatrix} \kappa_h \\ \kappa_v \end{Bmatrix} \tag{28}$$

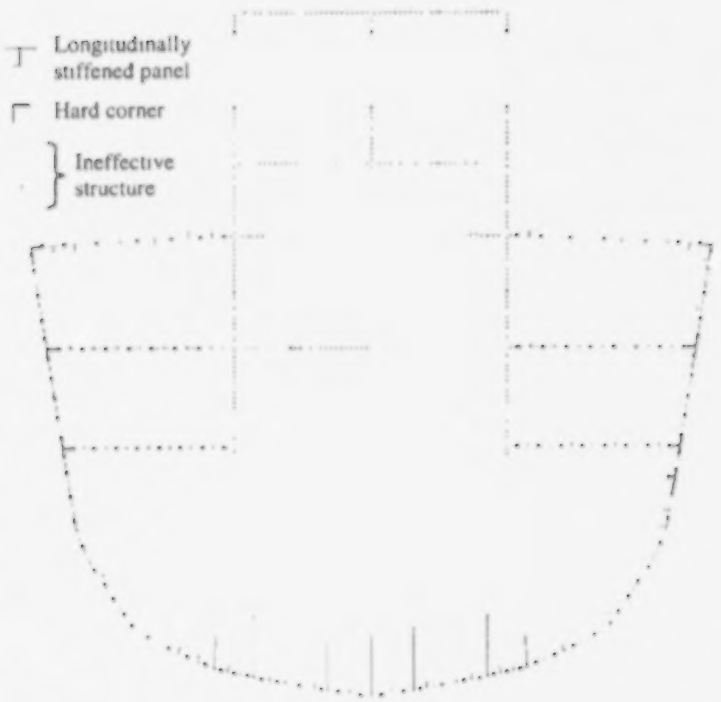

Figure 10: *Warship cross-sectional model subdivided into structural units.*

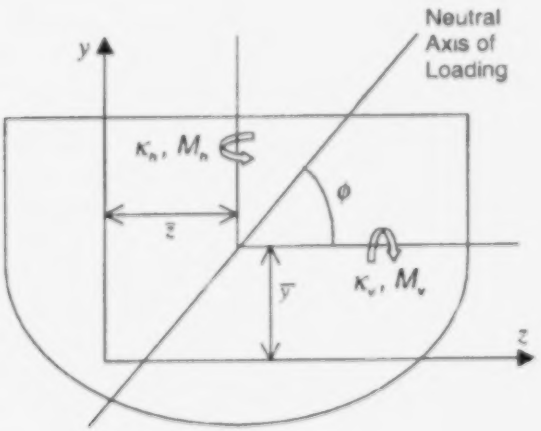

Figure 11: *Cross section orientation showing the direction of curvature loading ϕ.*

P517010.PDF [Page: 38 of 91]

with M_h and M_v representing the horizontal and vertical bending moments. In general, the moment-curvature relationship is nonlinear, so that the sectional rigidities D_{hh}, D_{hv}, and D_{vv} are functions of the curvature. The sectional rigidities can be calculated with the formula

$$D_{hh} = \sum_{i=1}^{n} (EA_e)_i (z_i - \overline{z})^2 \tag{29}$$

$$D_{hv} = \sum_{i=1}^{n} (EA_e)_i (y_i - \overline{y})(z_i - \overline{z}) \tag{30}$$

$$D_{vv} = \sum_{i=1}^{n} (EA_e)_i (y_i - \overline{y})^2 \tag{31}$$

where y_i, z_i are the vertical and horizontal positions of a structural unit, and $\overline{y}$, $\overline{z}$ define the current centroidal position of the section. In these expressions, E is the elastic modulus of the material and A_e is the effective cross-sectional area of unit i. The latter term is used to account for non-linear behaviour such as yielding and collapse. It can be conveniently represented as

$$A_e = A\eta \tag{32}$$

where A is the unit cross-sectional area and η is a reduction factor. This represents the unit's deviation from perfectly elastic behaviour, and can be obtained directly from the normalised load-shortening curve for the unit by

$$\eta = \frac{\overline{\sigma}}{\overline{\epsilon}} = \frac{\sigma/\sigma_y}{\epsilon/\epsilon_y} \tag{33}$$

where ϵ, σ are the average longitudinal strain and stress in the unit, and σ_y and ϵ_y are the yield values of the material. Imperfections and inelastic buckling effects cause η to be less than one through the whole compressive range.

The centroidal position is calculated by the equations

$$\overline{y} = \frac{\sum y_i (EA_e)_i}{\sum (EA_e)_i} \qquad \overline{z} = \frac{\sum z_i (EA_e)_i}{\sum (EA_e)_i} \tag{34}$$

Because of the dependence of A_e on the centroidal position, these equations have to be used iteratively until an acceptable degree of accuracy is achieved.

Moment-curvature analysis can be programmed as shown Figure 12. The iterative process is carried out until the absolute curvature reaches some predefined maximum value. Alternatively, the process can be carried out for a set number of iterations.

P517010.PDF [Page: 39 of 91]

1. $\kappa' = 0$; $\Delta\kappa = \{\Delta\kappa_h \; \Delta\kappa_v\}^T$;

2. $\kappa = \kappa'$;

3. $\kappa' = \kappa + \Delta\kappa$;

4. Update unit states, $\overline{y}$, $\overline{z}$, and D';

5. Compute $M' = D'\kappa'$;

6. Return to Step 2 and repeat until $\|\kappa'\| = \kappa_{max}$.

***Figure 12:** Algorithm for bi-axial moment-curvature analysis.*

4.2 Bi-Axial Static Strength

In bi-axial strength analysis, a bending moment load is applied incrementally in a given direction until the ultimate value is achieved. This approach involves some additional complication, but it has certain advantages, as will be explained in the next section.

The angle ϕ in Figure 11 is now used to define the direction of moment loading. Thus, a moment increment vector can be defined as

$$\Delta M = \{\Delta M_h \; \Delta M_v\} = \|\Delta M\|\{\sin\phi \; \cos\phi\} \tag{35}$$

in which it can be seen that the ratio of horizontal to vertical moment increments is to be held constant throughout the iterations.

Suppose that an applied moment M produces a curvature of κ in a section with bending rigidity D. An incremental moment ΔM will result in an increment to the curvature of

$$\Delta\kappa = \left\{ \begin{array}{c} \Delta\kappa_h \\ \Delta\kappa_v \end{array} \right\} = [D]^{-1}\Delta M \tag{36}$$

where $[D]$ is the matrix of sectional rigidities given in (28), evaluated for current stress/strain states of the units and the current section properties. Based on this calculated curvature increment, an updated curvature is obtained as $\kappa' = \kappa + \Delta\kappa$. This in turn can be used to update the neutral axis position and the matrix of sectional rigidities.

If $[D']$ denotes the updated section rigidity, the updated bending moment vector is given by $M' = [D']\kappa'$. When structural units respond non-linearly, the updated moment M' will differ from the target value $M + \Delta M$. Since the target value can be expressed as

$$M + \Delta M = D(\kappa + \Delta\kappa) = D\kappa', \tag{37}$$

P517010.PDF [Page: 40 of 91]

1. $\kappa = 0$; $M' = 0$;
2. $\Delta M' = \Delta M = \{\Delta M_h \; \Delta M_v\}^T$;
3. $M = M'$;
4. $\Delta\kappa = D^{-1}\Delta M'$;
5. $\kappa' = \kappa + \Delta\kappa$;
6. Update unit states, $\overline{y}$, $\overline{z}$, and D';
7. Compute $M' = D'\kappa'$;
8. $\Delta M' = \Delta M - (D' - D)\kappa'$
9. Return to Step 3 and repeat until $\|M'\| < \|M\|$.

***Figure 13:** Algorithm for bi-axial static strength analysis.*

the difference between the updated moment and the target value is given by

$$\Delta M_{err} = M' - (M + \Delta M) = (D' - D)\kappa' \tag{38}$$

It can be seen that this moment increment error is due to the change in the sectional rigidity over the $\Delta\kappa$ interval.

This error can be corrected for in the next iteration by subtracting the error increment from the original increment ΔM, thus producing an adjusted increment vector given by

$$\Delta M' = \Delta M - \Delta M_{err} = \Delta M - (D' - D)\kappa' \tag{39}$$

Using the adjusted moment increment keeps the applied moment in the intended direction in the event of an uneven or unsymmetric collapse process.

The procedure for evaluating bi-axial static strength is given in Figure 13. The iterative process is carried out until the applied moment can no longer be increased in the direction of loading. This condition is expressed by the inequality in Step 9.

4.3 Interaction Curves

Bi-axial moment-curvature or bi-axial strength analysis, if applied over the full range of loading directions, can be used to generate an envelope of ultimate bending moments, known as an interaction curve, defining the safe limit of operation at a given section. In most situations, it is acceptable to use either bi-axial moment-curvature or bi-axial strength analysis to determine the points of an interaction

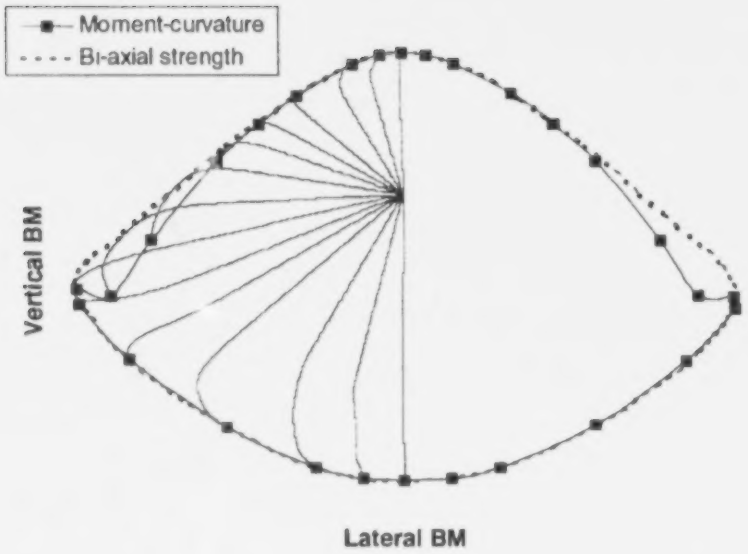

Figure 14: *Interaction curve obtained with bi-axial moment-curvature analysis.*

curve; however some instances arise where moment-curvature analysis gives rise to inaccurate results, as will be explained in the following.

Figure 14 shows an interaction curve generated for the HALIFAX class vessel at midships. Each point of the curve, represented by a square, was calculated by a moment-curvature analysis. The trace lines radiating from the centre of the plot and terminating at the squares indicate bi-axial bending moment values generated prior to failure by individual moment-curvature analyses. These show that very substantial changes in the vertical to lateral bending moment ratio occur during each analysis. Moreover, some segments of the trace lines actually extend outside the interaction curve. This is a contradiction, since it suggests that valid, pre-failure bending moments can exist beyond the apparent safe limit.

By comparison, the interaction curve shown in Figure 15 was determined using bi-axial strength analysis at each point. Here the trace lines are straight, as is enforced by the adjusted moment increments. The distortion around the lateral limits of the curve in Figure 14 is not present here. The interaction curve of Figure 15 appears in Figure 14 as a broken line, where it can be seen that the curved trace lines do not extend beyond the broken line at any point. In fact, the broken line forms an envelope around the curved trace lines. Clearly, bi-axial strength analysis provides a superior interaction curve in this situation.

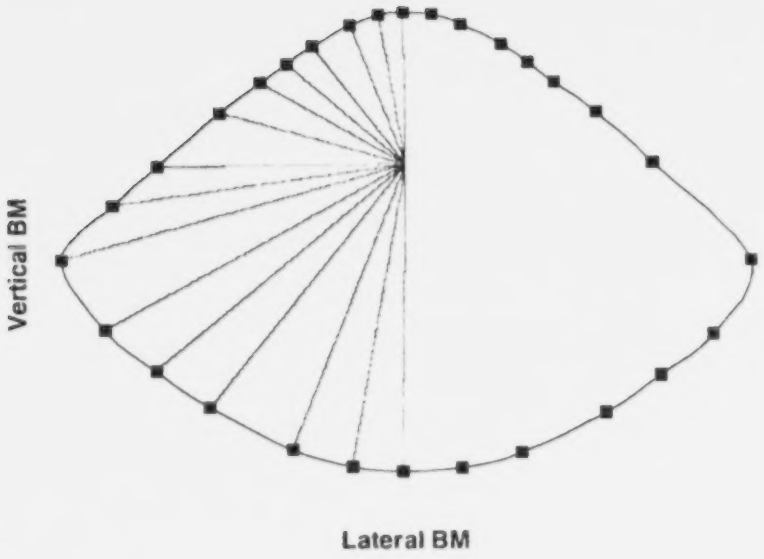

Figure 15: *Interaction curve obtained with bi-axial strength analysis.*

The distortion in Figure 14 is the result of half-framing in the hull bottom of the HALIFAX class structure. Under extreme lateral bending moments, the structure collapses in an asymmetric fashion, with the resisting compressive loading shifting down to the stronger panels in the bottom. This explains the downward curving trace lines in Figure 14.

5 Implementation

The ultimate strength procedures described above have been recently implemented and tested in an in-house development at DREA. The code RESULTS represents a significant step forward from the earlier ULTMAT code, in that both bi-axial moment-curvature and bi-axial strength can be performed, and that interaction curves and other types of analysis have been integrated into a single application. The code was written in C++ using principles of object-oriented programming.

Although it is a development separate from ULTSAS, RESULTS is designed to share cross-section data formats and load-shortening curve databases with that code, and thus maintain continuity with previous developments.

Other aspects of the development are described in the following. A user's guide giving a detailed description of the programme's analysis options and input data

format is given in Annex B.

5.1 Analysis Types

The six types of analysis available to the RESULTS user are listed as follows:

1. Bi-axial moment-curvature analysis
2. Bi-axial static strength prediction
3. Interaction curve analysis
4. Hog and sag analysis
5. First-yield moment prediction
6. Plastic moment prediction

The first three have been discussed extensively in the preceding discussion of the theory. Hog and sag analysis is just the moment-curvature analysis type specialised to the two vertical bending cases. This has been provided in the programme for the convenience of the user. First-yield analysis is for determining a bi-axial moment that produces a first-yield condition in a defined loading direction. Plastic moment analysis is for determining the bi-axial moment resulting from a fully developed plastic moment condition in a section, neglecting lateral instability of the structural units. The latter two analysis types are intended primarly for reference and data checking purposes.

5.2 Cross Section Data Format

RESULTS accepts cross section definitions that have already been grouped into structural units. Two formats are currently readable: the ULTMAT format generated by ULTSAS, and a more generic format. The ULTMAT format is restricted to use with longitudinally stiffened panels and corners. It also does not record the A_s/A ratio for stiffened panels, or the level of imperfection. These shortcomings are addressed by the generic format, which is given in Annex B.2. The generic format includes all the information currently used to define structural units, and is easily expandable to incorporate additional structural unit types and properties. In the generic format, structural unit imperfections are restricted to one of three predefined levels: slight, average, and severe, with average being the default.

A further refinement is that, unlike the ULTMAT and NS94 formats, the material properties are defined separately from structural units in the RESULTS generic format. Each structural unit is associated to a material through a string identifier. This

is a much more flexible arrangement, as it allows a cross section's material properties to be quickly adjusted, and enables new material models to be incorporated without affecting the cross-section definition.

5.3 L-S Databases

RESULTS reads directly from either the HALIFAX class longitudinal database or the NS94C/D bi-linear database, both of which are included with the ULTSAS software. The user may also supply additional L-S curves and associate them with specific structural units in the model. This feature was also provided with ULTSAS. At present, neither of the design equations for calculating L-S behaviour for calculating L-S behaviour presented in Section 3.6 have been implemented.

For the HALIFAX class longitudinal database, the user can choose between sets of curves generated with either end-to-end or centre-to-centre stiffened panel models. Once this choice is made, the programme reads all the curves necessary for interpolating the L-S behaviour of the structural units. Interpolation is carried out for β, λ, and A_s/A, where the information is available. Interpolation is not performed for imperfection levels. Instead, a structural unit's level of imperfection is matched to curves in the database with the same imperfection level.

6 Comparison with Test Results

6.1 Summary of Previous Test Measurements

In 1981, Dow et al. [34] reviewed previous experiments related to ultimate hull girder strength. Data from real ships were limited to studies of two American destroyers (PRESTON and BRUCE) in 1930 and a British destroyer in 1950 (ALBUERA). All of these ships had rivetted construction, and therefore are of limited use in understanding modern warships. In 1980, the VLCC *Energy Concentration* suffered a hull girder failure while discharging her cargo. Rutherford and Caldwell [35] used the known loading conditions, weight distribution, and corrosion damage to determine the ultimate bending moment.

Lacking data from real ships, ultimate strength testing has focussed on small scale box girder structures. Dowling [36], Reckling [37], Nishihara [38], Mansour et al. [39], and Akhras [40] all tested welded box girder structures that were representative of ship structures. More realistic ship structure behaviour was achieved in a test by Dow [22] using a 1/3 scale model of a British LEANDER class frigate.

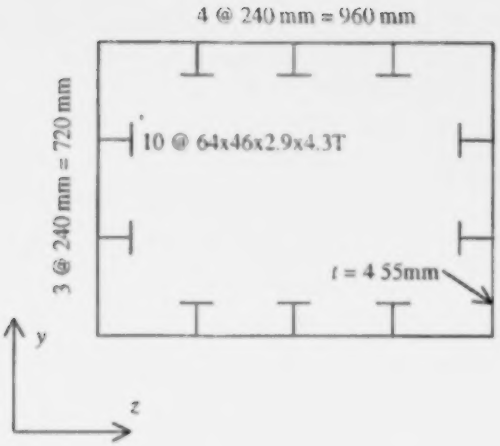

***Figure 16:** Akhras box girder cross section [40].*

6.2 Comparison with Akhras Box Girder

Akhras [40] performed ultimate and residual strength tests on a box girder structure with the cross section illustrated in Figure 16. The tests performed by Akhras gave an ultimate strength value of 1237.5 kNm (see Table 5) for vertical bending (i.e., bending about the z axis). This experimental value is used here to validate the progressive collapse method implemented in RESULTS.

The cross-sectional model of the box girder is subdivided into ten stiffened panel and four corner elements. The geometric distortions measured in the Akhras box model [40] most closely correspond with a plating distortion level of $0.1\beta^2 t$ (see Table 1). Thus, a "slight" imperfection level was used with the stiffened panel units.

Figure 17 shows moment-curvature plots obtained with the RESULTS programme using the three available LSC databases. The ultimate strengths obtained from these analyses are given in Table 5. The result obtained with the end-to-end LSC database is only 1.5% different from the measured value. Figure 18 gives the interaction curves obtained with the same three LSC databases. Because of the symmetry in the structure, only one quarter of each of the curves is shown. Some of the ultimate strength values obtained in vertical bending differ from those in the interaction curves. This is due to a deficiency in bi-axial strength analysis that occurs when a double local maxima occur in the moment-curvature response. In this case, double maxima appear in the results obtained with the two CPF LSC databases, as shown in Figure 17. Bi-axial strength analysis can iterate as far as the first maximum (approximately a plateau) but is unable to reach the second, true maximum. As a

Table 5: *Ultimate Strengths for Akhras Box Girder*

Source	Ultimate Strength (kNm)
Experiment	1237.5
ResUltS (End-to-End DB)	1220.3
ResUltS (Centre-to-Centre DB)	1198.4
ResUltS (NS94 DB)	1261.2
FE (ANSYS)	1252.6

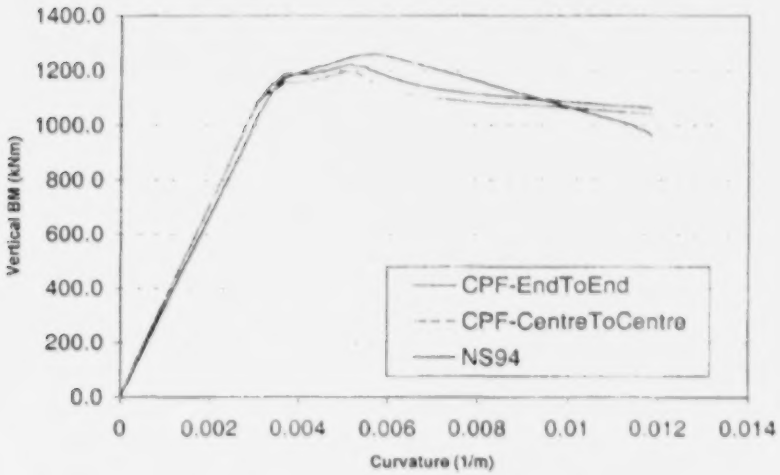

Figure 17: *Box girder moment-curvature response in vertical bending predicted by RESULTS.*

result, points in the two interaction curves corresponding to vertical bending are visibly lower than the ultimate strengths obtained with moment-curvature analysis. When the NS94 database is used only one maximum occurs in the response, and the bi-axial strength analysis finds the correct ultimate strength.

The double maxima in Figure 17 are a progressive collapse effect, the first maximum corresponding to the collapse of the compression flange units, and the second to the collapse of the web units. The small number of units in the cross section enables these two events to be clearly distinguished. In cross sectional models of real ships with a hundred or more structural units, separate collapse events are smeared out in the response, and a single overall peak results.

Further validation was performed with non-linear finite element analysis of a three-

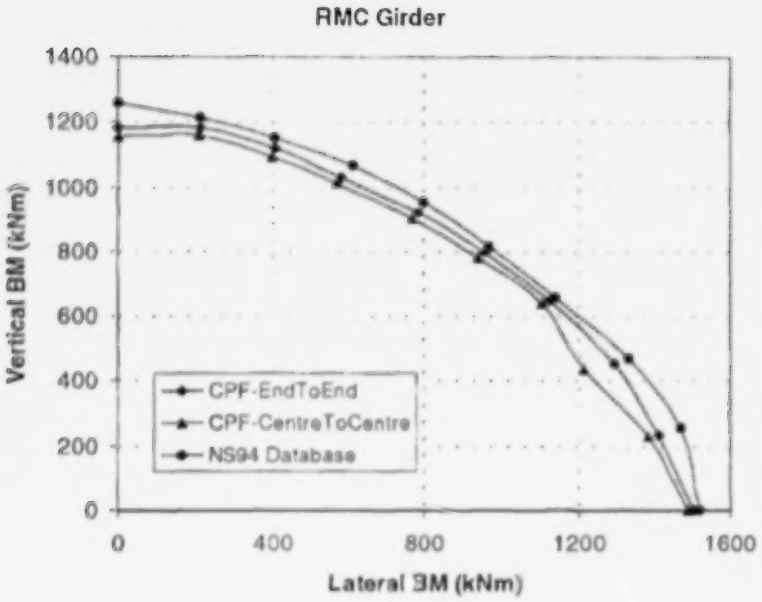

Figure 18: *Box girder interaction curves predicted by RESULTS.*

dimensional model of the box girder. The FE model is shown in Figure 19, and is a simplified version of the girder used in the Akhras tests. A four-point bending load is applied with displacement constraints at the locations shown. This ensures that a pure moment loading is applied on the refined, central section of the girder. Geometric distortion was added to the plating and stiffeners on the compression flange in the test section. The amount of distortion was about three times larger (in amplitude) than the actual distortions reported in the experimental work. It was found that the non-linear algorithm in ANSYS could not converge on a solution with smaller amounts of distortion. To compensate for this excess distortion, residual stresses were not included in the analysis.

The after-collapse deformed shape of the compression flange plating and stiffeners is shown in Figures 20 and 21. Note that the deformed shape is not symmetric with respect to the middle cross-section, although the model, loads and distortions are symmetric. The ultimate strength obtained with FEA is only 1.2% higher than the experimental result. The deformed shape of the plating on the compression flange and the girder webs is very similar to what was observed in the Akhras tests [40].

Figure 22 compares the moment-curvature response obtained with PCM, finite element analysis, and the Akhras experimental results. The FEA and PCM curves match reasonably well. The slopes of the curves in the linear region are somewhat

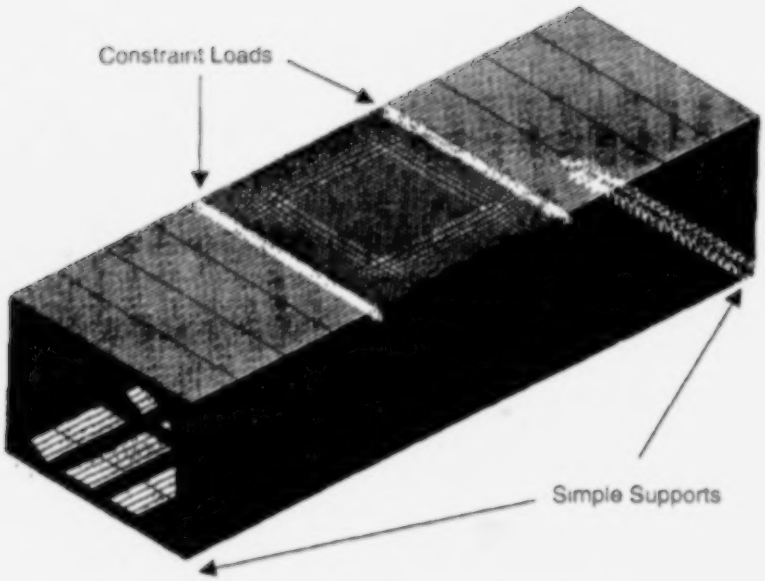

Figure 19: *Finite element model of box girder under four-point bending.*

different, and the FEA results give significantly higher moments in the post-collapse region. Also, there is no sign of the double maxima in the FEA results, which suggests that this effect is more likely an artifact of the cross-sectional modelling assumptions in PCM than it is a real phenomenon.

The moment-curvature response was not directly measured by Akhras. Instead, he measured the force and displacement of the loaded sections. From this it is easy to determine the moment in the test section, but determining the curvature is more problematic. The average curvature in the test section can be obtained from the difference of the rotations of the sections at either end. These rotations were obtained from the measured deflections and by assuming that beam theory is valid in the outer sections of the girder. The resulting moment-curvature response puts the measured ultimate strength at a curvature that is about fifty percent greater than what is predicted with FEA and PCM.

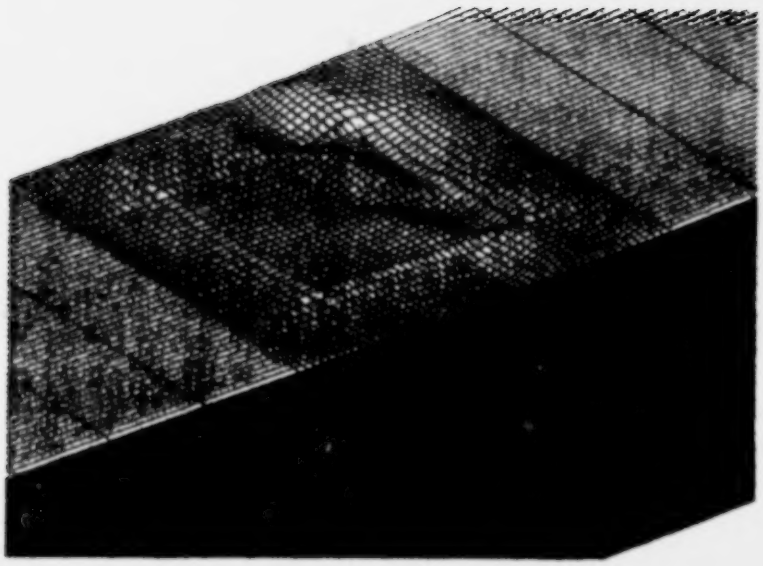

Figure 20: *Deformed shape of box girder structure in post-collapse region.*

Figure 21: *Deformed shape of box girder structure in post-collapse region (interior).*

P517010.PDF [Page: 50 of 91]

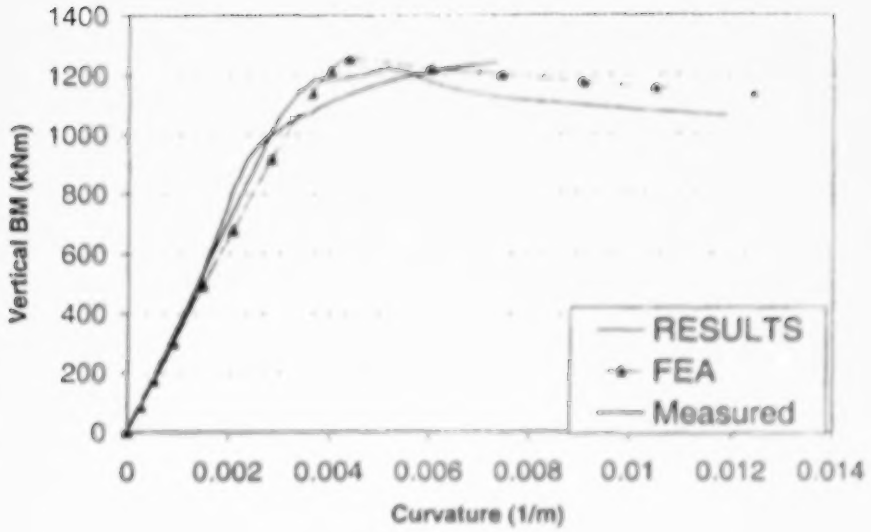

***Figure 22:** Vertical moment-curvature response of box girder structure.*

7 Application to Canadian Warships

In a recent study a variety of ultimate strength results obtained from the ULTSAS software for three CF warship designs are described [9]. The results presented here are primarily concerned with validating the ultimate strength analysis procedures recently implemented in the RESULTS software, as described in the previous sections, as well as to present some results of warship damage scenarios of interest to the ongoing ISSMM development [11].

7.1 Explosion Damage Case

The HALIFAX class hull section in Figure 23 was subject to a hypothetical explosion damage scenario on the starboard side of the main deck near midships. A three-metre wide section of structure is affected, resulting in the loss of five longitudinal panels.

Strength reduction can be expected at cross-sections that are directly damaged, due to loss of structure, and also at nearby undamaged cross-sections because the main deck is no longer longitudinally continuous, and therefore not fully effective in resisting bending moments. In this case since the damaged section is amidships, which is the most significant region of the ship in the context of hull-girder strength, the effect of the damage can be evaluated in this region alone. A cross-sectional

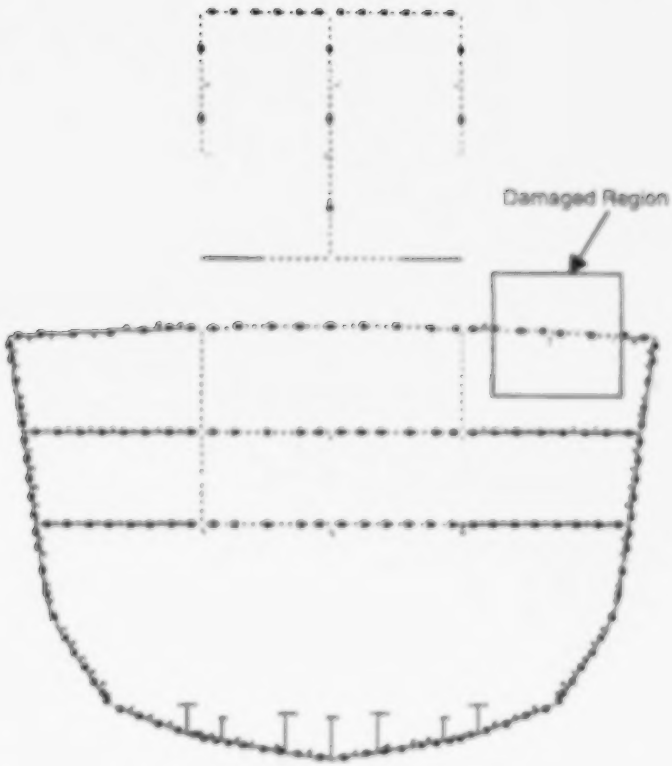

Figure 23: *HALIFAX class hull section, with damage region indicated.*

model is shown in Figure 23, indicating the region where damage occurs. The damaged is modelled as the disabling of five longitudinal units in the starboard main deck, which is indicated by broken lines. Other structure, notably the superstructure, longitudinal bulkheads, and the inboard portion of the decks, is disabled because it is not longitudinally effective. Interaction curves for the damaged and undamaged sections are given in Figure 24. Good agreement is obtained between NS94B and RESULTS curves. These indicate an 18% reduction in sag strength, and an 11% reduction in hog strength. The effect of the damage is to shrink the extent of the interaction curve, and also to rotate it. The rotation is the result of the asymmetry in the damaged section.

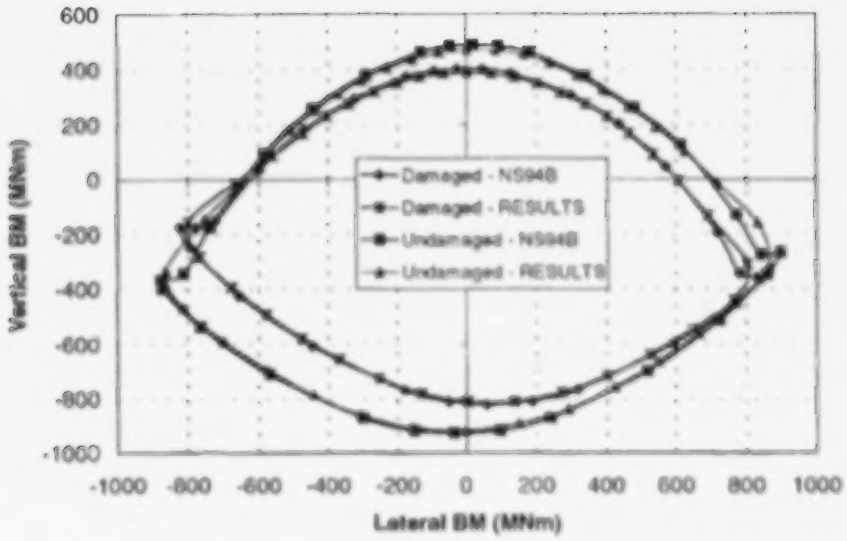

Figure 24: *Interaction curve for explosion damage test case.*

7.2 Collision Damage Case

The collision damage case examined here introduces indentation in the top three longitudinal units of the sheer strake and in the hard corner unit at the juncture of the main deck and the sheer strake. It also severely damages the outermost longitudinal unit in the main deck. The following two approaches to modelling the damage are explored here: (1) the deformation of the affected structure; and (2) the loss of structure in the affected areas. In the first approach deformation of the panels affects only their compressive strengths, whereas in the second approach the loss of structure affects both tensile and compressive strengths.

Figure 25 shows the cross section and the region affected by the collision damage. Considering the first damage modelling case, the average deformation in three affected sheer strake longitudinal units are, moving from the deck downward, 300, 200 and 25 mm, respectively. Load-shortening curves for all three were recalculated with ULTSAS using these damage values. It was found that the two most severely damage longitudinals have almost no remaining compressive load-carrying capacity, while the strength of the third panel is lowered by about 10%. The indentation in the hard corner unit is large enough to sever the unit, and so it too can be removed from the analysis. The affected longitudinal unit on the main deck has its outboard plating severely damaged, but the stiffener and inboard plating is assumed to be unaffected. This has the effect of reducing the effective width of the unit's attached

plating by half.

Ultimate strength analysis is performed with other ineffective structure disabled in the cross section. This includes the whole superstructure, and the deck and bulkhead structure beneath the superstructure. Figure 26 gives the damaged and undamaged interaction curves. These results show that the damage reduces the strength of the hull by about 10% in sag. The bi-axial strengths are reduced in the range of 5 to 10% in the top-side and port-side quadrant. The damage has little effect on the hog strength or on the bi-axial strength in the starboard quadrants.

The second damage modelling case is now considered in which the three affected sheer strake stiffened panel units are disabled from the analysis. The corner and deck stiffened panel units are treated in the same way as in the deformation case. The interaction curve obtained with this approach is shown in Figure 27, and is compared with the curves for the undamaged and deformation damage. As expected, the removal of the damaged structure affects both the hog and sag strengths. Moreover, the change in the damaged hull strength due to the removal of the sheer strake panels is entirely attributable to the loss of the tensile strength of these panels.

8 Conclusion

This Memorandum has described the recent re-development of DREA's ultimate strength code. The damage scenario examples that have been provided show that the programme is capable of performing bi-axial strength and moment curvature analysis required for the ISSMM Software Tool (IST). The new code is to be used as the analysis code in the ultimate strength module of the IST.

The approach to ultimate strength assessment used by the RESULTS code assumes significant simplification of the hull-girder failure process. Failures are treated as single load cycle events in which bending moment loads are applied statically to the hull. Developing capabilities for assessing residual strength, i.e., the strength of the hull in a load cycle subsequent to a partial structural failure, would enable a more realistic multi-cyclic failure process to be evaluated. One approach for treating the multi-cyclic problem is through extension of the conventional load shortening curves to include not just one, but several compressive and tensile load branches. Further work is planned at DREA in this direction using either the pre-calculated LSC databases described in Section 3.4 or design equations such as those discussed in Section 3.6.

In modelling of structural cross sections, some simplification of the structure is unavoidable. As was noted in the examples of Section 7, much of the cross-sectional structure is disabled as ineffective in resisting bending moment loads. The heuristic

P517010.PDF [Page: 54 of 91]

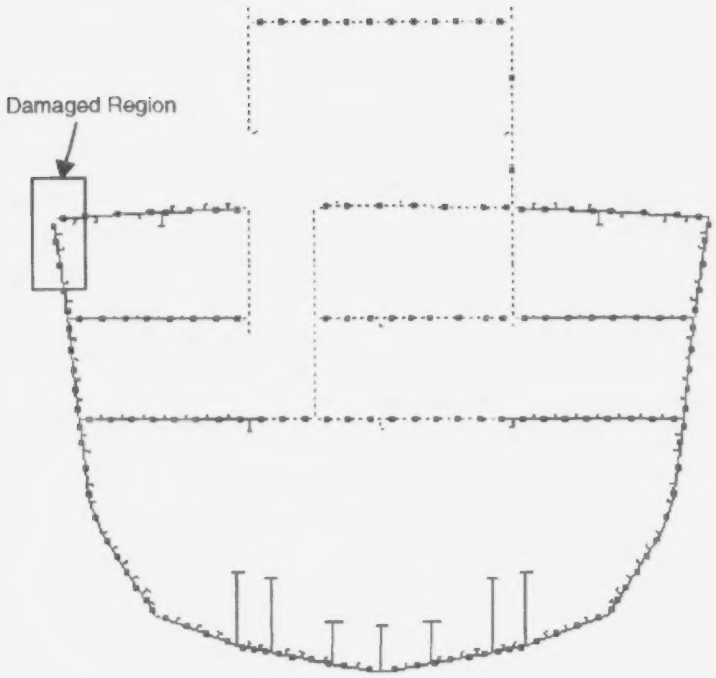

Figure 25: *Cross section with collision damage region indicated.*

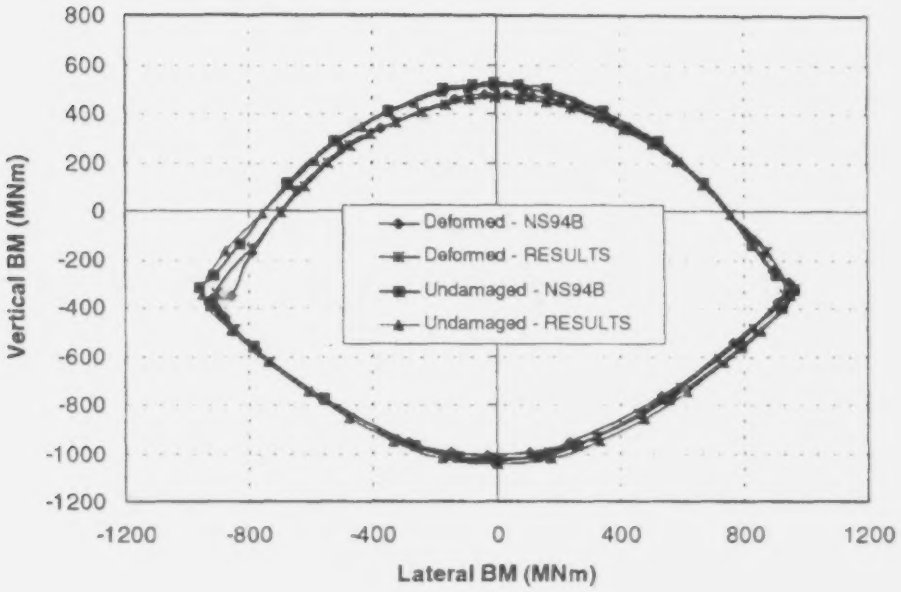

Figure 26: *Interaction curve for collision deformation damage case.*

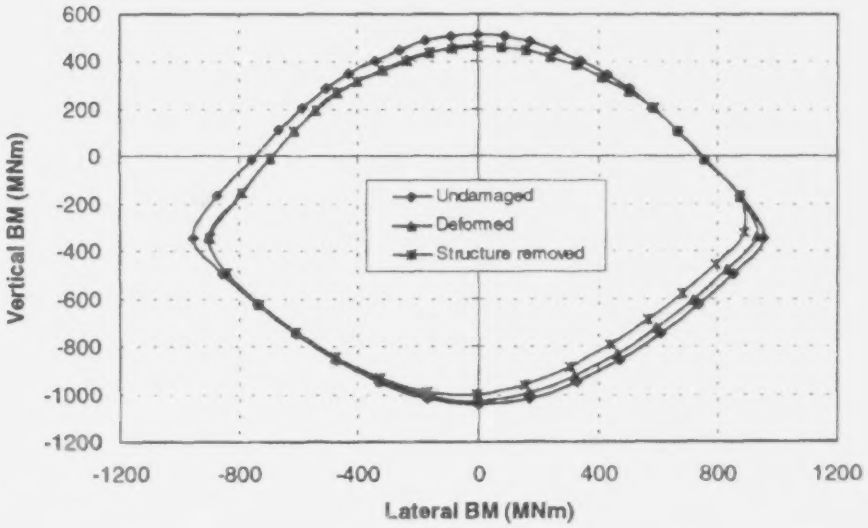

Figure 27: *RESULTS interaction curves for two collision damage modelling approaches.*

P517010.PDF [Page: 56 of 91]

method for identifying ineffective structure introduces significant uncertainty in a longitudinal strength calculation. Other sources of uncertainty arise in the modelling of load carrying characteristics of structural units, especially in the treatment of weld-induced imperfections and compressive behaviour of hard corner and deep girder structure. A probabilistic or reliability type approach is needed to quantify the effects of these and other, more typical, uncertainties such as scantlings and material properties. The development of such a capability in the RESULTS programme is planned for the near future.

References

1. Pegg, N. G. and Cox, P. (1985). ULTMAT - A Program for Predicting the Ultimate Strength of Ship Cross Sections. (Technical Communication 85/313). Defence Research Establishment Atlantic.

2. Smith, C. S. and Dow, R. S. (1986). Ultimate Strength of a Ship's Hull under Biaxial Bending. (ARE TR 86204). Admiralty Research Establishment.

3. Dow, R. S. (1997). NS94C/D Ultimate Strength Design Method for Ships. (DRA/SS/SSSV/CR97215). Defence Research Agency Dunfermline.

4. Dow, R. S., and Smith, C. S. (1986). FABSTRAN: A Computer Program for Frame and Beam Static and Transient Response Analysis. (ARE TR 86205). Admiralty Research Establishment.

5. Adamchak, J. C. (1984). An Approximate Method for Estimating the Collapse of a Ship's Hull in Preliminary Design. *Ship Structure Symposium '84*. SNAME. 37–61.

6. Jiang, L., and Chernuka, M. (2000). Incorporation of UK NS94 Ultimate Strength Analysis in MGDSA, Part I: Engineering Considerations. (DREA CR 2000-112). Martec Limited.

7. Lichodzijewski, M., and Jiang, L. (2000). Incorporation of UK NS94 Ultimate Strength Analysis in MGDSA, Part II: Software Considerations. (DREA CR 2000-113). Martec Limited.

8. Lichodzijewski, M., and MacAdam, T. (2000). Ultimate Strength Application Version 1.0 Users Manual. (DREA CR 2000-114). Martec Limited.

9. Smith, M. J. and Pegg, N. G. (2000). Automated Assessment of Ultimate Longitudinal Strength of Ship Hulls. (Technical Memorandum TM 2000-143). Defence Research Establishment Atlantic.

P517010.PDF [Page: 57 of 91]

10. Smith, C. S. (1977). Influence of Local Compression Failure on Ultimate Longitudinal Strength of a Ships Hull. Proceedings, International Symposium on Practical Design in Shipbuilding, Tokyo 73–79.

11. Pegg, N. G. (1999). Development of the ISSMM Software Tool for Residual Strength Assessment of Ship Structures. (DREA TM 1999-055). Defence Research Establishment Atlantic.

12. Caldwell, J. B. (1965). Ultimate Longitudinal Strength, *Trans. RINA*. 107, 411–230.

13. Mansour, A. E., and Thayamballi, A. (1980). Ultimate Strength of a Ship's Hull Girder Plastic and Buckling Modes. (SSC-299). Ship Structure Committee.

14. Paik, J. K., and Mansour, A. E. (1995). A Simple Formulation for Predicting the Ultimate Strength of Ships. *Journal of Marine Science and Technology*. 1, 52–62.

15. Rahman, M. K., and Chowdhury, M. (1996). Estimation of Ultimate Longitudinal Bending Moment of Ships and Box Girders. *Journal of Ship Research*, 40 (3) 244–257.

16. Hughes, O. F. (1983) Ship Structural Design. Chap. 14. New York: John Wiley & Sons.

17. Gordo, J. M., Guedes Soares, C., and Faulkner, D. (1996). Approximate Assessment of the Ultimate Longitudinal Strength of the Hull Girder. *Journal of Ship Research*, 40 (1), 60–69.

18. Gordo, J. M., Guedes Soares, C. (1996). Approximate Method to Evaluate the Hull Girder Collapse Strength. *Marine Structures*, 9, 449–470.

19. Gordo, J. M., Guedes Soares, C. (1993). Approximate Load Shortening Curves for Stiffened Plates under Uniaxial Compression. *Integrity of Offshore Structures—5*. D. Faulkner et al., Eds. EMAS. 189–211.

20. Hansen, A. M. (1996). Strength of Midship Sections. *Marine Structures*. 9, 471–494.

21. Chen, Y-K., Kutt, L. M., Piaszczyk, C. M., and Bieniek, M. P. (1983). Ultimate Strength of Ship Structures, *SNAME Transactions*. 91, 149-168.

22. Dow, R. S. (1991). Testing and Analysis of a 1/3-Scale Welded Steel Frigate Model. *Advances in Marine Structures—2*. C. S. Smith and R. S. Dow, Eds. London: Elsevier, 749–773.

P517010.PDF [Page: 58 of 91]

23. Ueda, Y. and Rashed, S. M. H., (1984). The Idealized Structural Unit Method and Its Application to Deep Girder Structures. *Computers & Structures*. 18 (2) 277–293.

24. Ueda, Y. and Rashed, S. M. H. (1991). Advances in the Application of ISUM to Marine Structures. Advances in Marine Structures - 2, C. Smith and R. S. Dow, Eds. London: Elsevier, 628-649.

25. Ueda, Y. and Yao, T. (1982). The Plastic Node Method: A New Method of Plastic Analysis. *Computer Methods in Applied Mechanics and Engineering*. 34, 1089-1104.

26. Bai, Y., Bendiksen, E., and Pedersen, P. T. (1993). Collapse Analysis of Ship Hulls. *Marine Structures*. 6, 485–507.

27. Faulkner, D. (1975). A Review of Effective Plating for Use in the Analysis of Stiffened Plating in Bending and Compression. *Journal of Ship Research*. 15(1), 1–17.

28. Chen, Q., Zimmerman, T. J. E., DeGeer, D. D., Kennedy, B. W. (1997). Strength and Stability of Stiffened Panel Components. (SSC-399). Ship Structures Committee.

29. Wallace, J. C., Jiang, L., and Chernuka, M. (1997). Generation of a Normalized Effective Stress-Strain Curve Database of Stiffened Panels for the Halifax Class Frigate. (Technical Report TR 97-39). Martec Limited. Halifax, Nova Scotia.

30. Jiang, L., and Chernuka, M. (1998). Continued Development of a Normalized Effective Stress-Strain Curve Database of Stiffened Panels for the Halifax Class Frigate. (Technical Report TR 98-08). Martec Limited. Halifax, Nova Scotia.

31. Martec Limited. (1997). VAST — Vibration and Strength Analysis. Version 7.2 User's Manual.

32. Smith, C. S., Anderson, N., Chapman, J. C., Davidson, P. C., and Dowling, P. J. (1992). Strength of Stiffened Plating under Combined Compression and Lateral Pressure. *Transactions of RINA*. 134, 131–147.

33. Jiang, L., and Chernuka M. W. (2000). Improved Nonlinear Solution Techniques in the VAST Finite Element Program. (DREA CR 2000-101). Martec Limited.

P517010.PDF [Page: 59 of 91]

34. Dow, R. S., Hugill, R. C., Clark, J. D., and Smith, C. S. (1981). Evaluation of Ultimate Ship Hull Strength. *Proceedings of the SNAME Extreme Loads Response Symposium*. 133–147.

35. Rutherford, S. E., and Caldwell, J. B. (1990). Ultimate Longitudinal Strength of Ships: a Case Study. *SNAME Transactions*, 90, 441-471.

36. Dowling, P. J., Chatterjee, S., Frieze, P. A., and Moolani, F. O. (1973). Experimental and Predicted Collapse Behaviour of Rectangular Steel Box Girders. Int. Conf. on Steel Box Girder Bridges, London.

37. Reckling, K. A. (1979) Preliminary Report on Box Girder Experiments, (included in Report of Committee II.2 on Non-linear Structural Response). *Proc. of 7th International Ship Structures Congress*, Paris.

38. Nishihara, S. (1984). Ultimate Longitudinal Strength of Midship Cross Sections. *Naval Arch. & Ocean Engng*, 22, 200–214.

39. Mansour, A. E., Yang, J. M., and Thayamballi, A. (1990). An Experimental Investigation of Ship Hull Ultimate Strength. *SNAME Transactions*, 90, 411-440.

40. Akhras, G. (1996) Determining the Ultimate Strength of Ship's Hulls. Unpublished Report. Royal Military College of Canada, Kingston.

P517010 PDF [Page: 60 of 91]

Annex A
Load-Shortening Curve Data

The following pages show comparisons of load-shortening curves obtained with two sets of finite element models and two sets of design equations. See Section 3.6 for a discussion.

P517010 PDF [Page: 61 of 91]

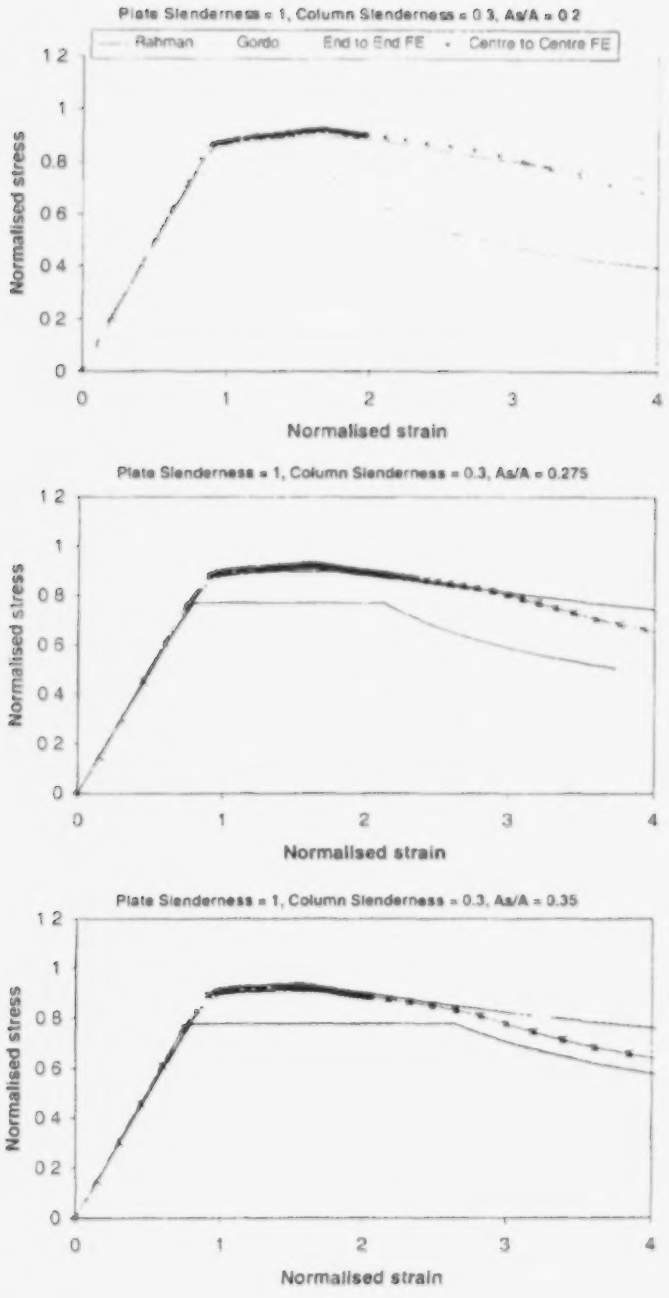
Plate Slenderness = 1, Column Slenderness = 0.3, As/A = 0.2
Rahman
Gordo
End to End FE
Centre to Centre FE
Normalised stress
Normalised strain
Plate Slenderness = 1, Column Slenderness = 0.3, As/A = 0.275
Normalised stress
Normalised strain
Plate Slenderness = 1, Column Slenderness = 0.3, As/A = 0.35
Normalised stress
Normalised strain

Figure A.1: *Curves for* $\beta = 1$ *and* $\lambda = 0.3$.

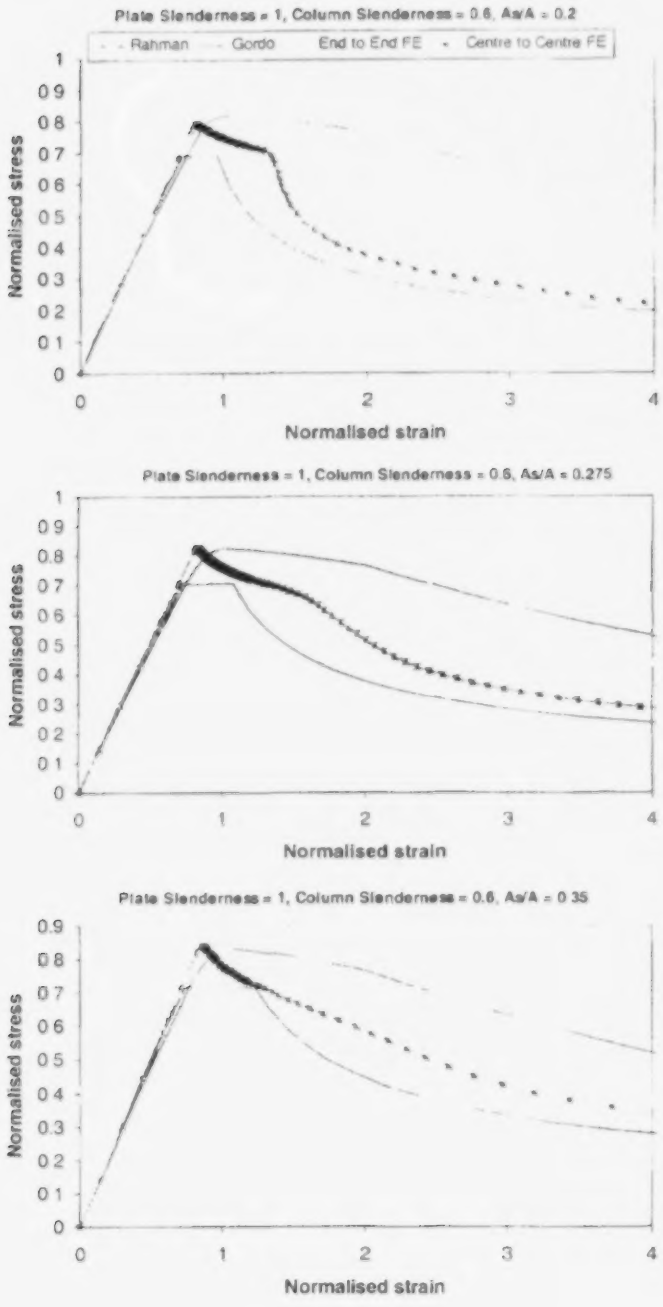
Plate Slenderness = 1, Column Slenderness = 0.6, As/A = 0.2
Rahman
Gordo
End to End FE
Centre to Centre FE
Normalised stress
Normalised strain
Plate Slenderness = 1, Column Slenderness = 0.6, As/A = 0.275
Normalised stress
Normalised strain
Plate Slenderness = 1, Column Slenderness = 0.6, As/A = 0.35
Normalised stress
Normalised strain

Figure A.2: *Curves for* $\beta = 1$ *and* $\lambda = 0.6$.

P517010.PDF [Page: 63 of 91]

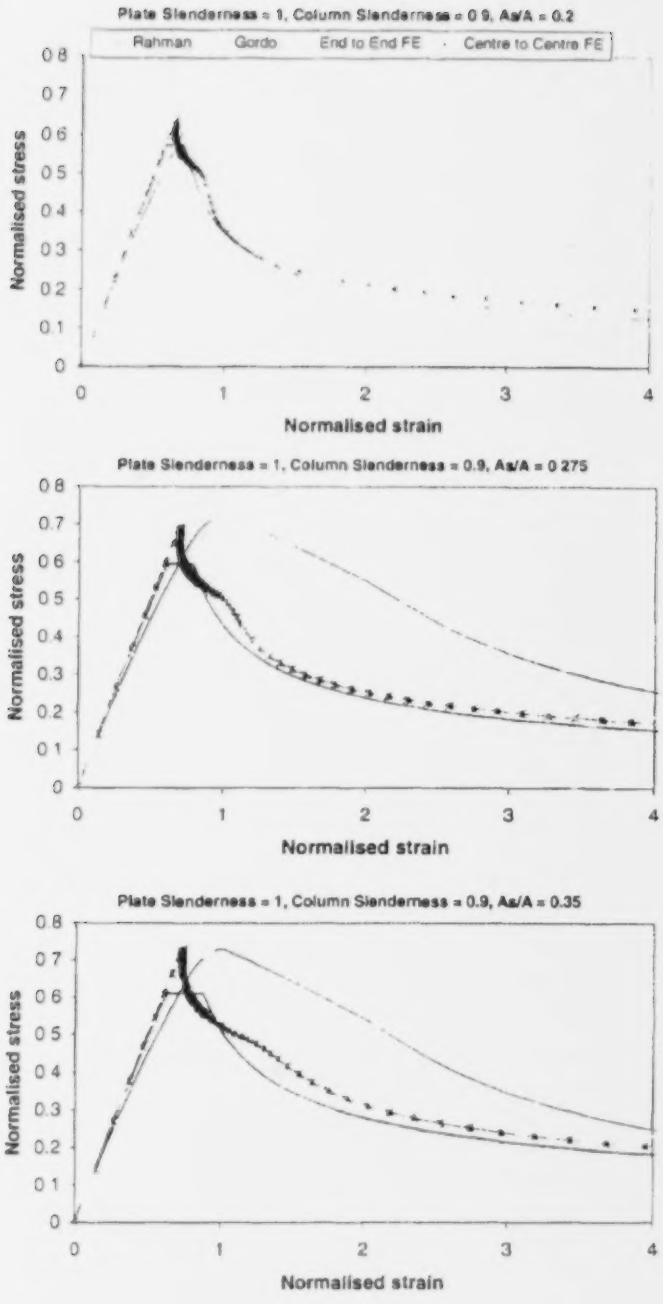
Plate Slenderness = 1, Column Slenderness = 0.9, As/A = 0.2
Rahman
Gordo
End to End FE
Centre to Centre FE
Normalised stress
Normalised strain
Plate Slenderness = 1, Column Slenderness = 0.9, As/A = 0.275
Normalised stress
Normalised strain
Plate Slenderness = 1, Column Slenderness = 0.9, As/A = 0.35
Normalised stress
Normalised strain

Figure A.3: *Curves for* $\beta = 1$ *and* $\lambda = 0.9$.

PS17010.PDF [Page: 64 of 91]

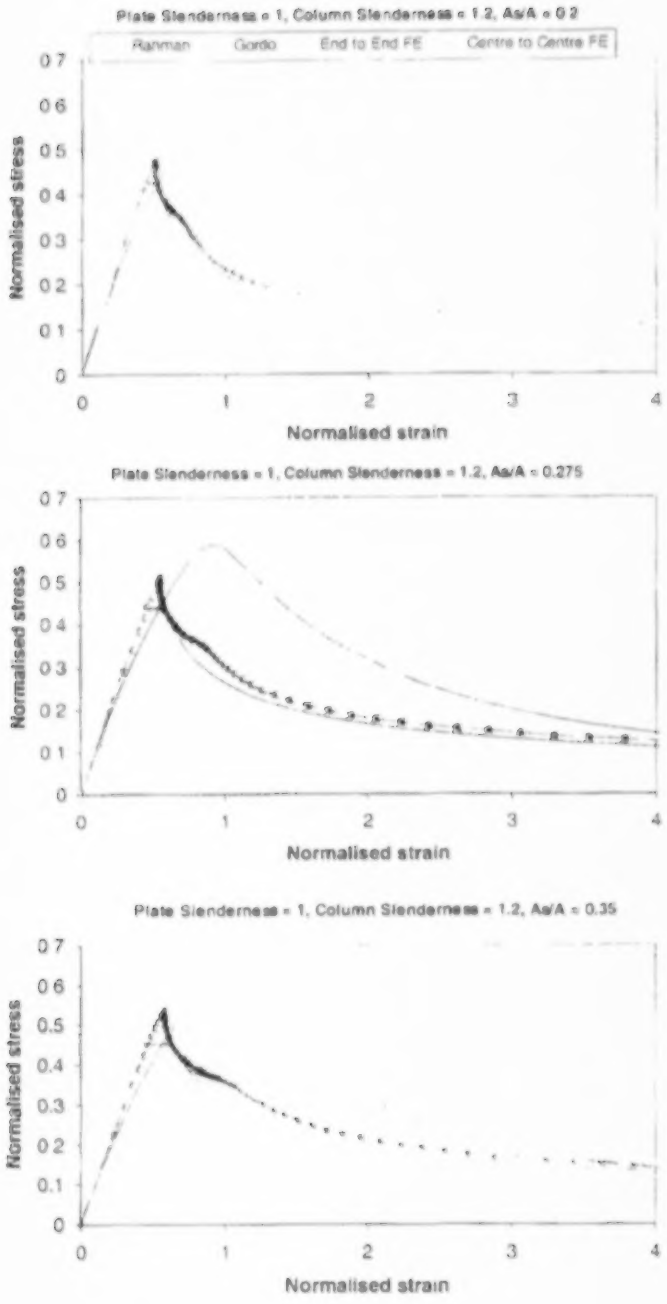
Plate Slenderness = 1, Column Slenderness = 1.2, As/A = 0.2
Ranman
Gordo
End to End FE
Centre to Centre FE
Normalised stress
Normalised strain
Plate Slenderness = 1, Column Slenderness = 1.2, As/A = 0.275
Normalised stress
Normalised strain
Plate Slenderness = 1, Column Slenderness = 1.2, As/A = 0.35
Normalised stress
Normalised strain

Figure A.4: *Curves for* $\beta = 1$ *and* $\lambda = 1.2$.

P517010.PDF [Page: 65 of 91]

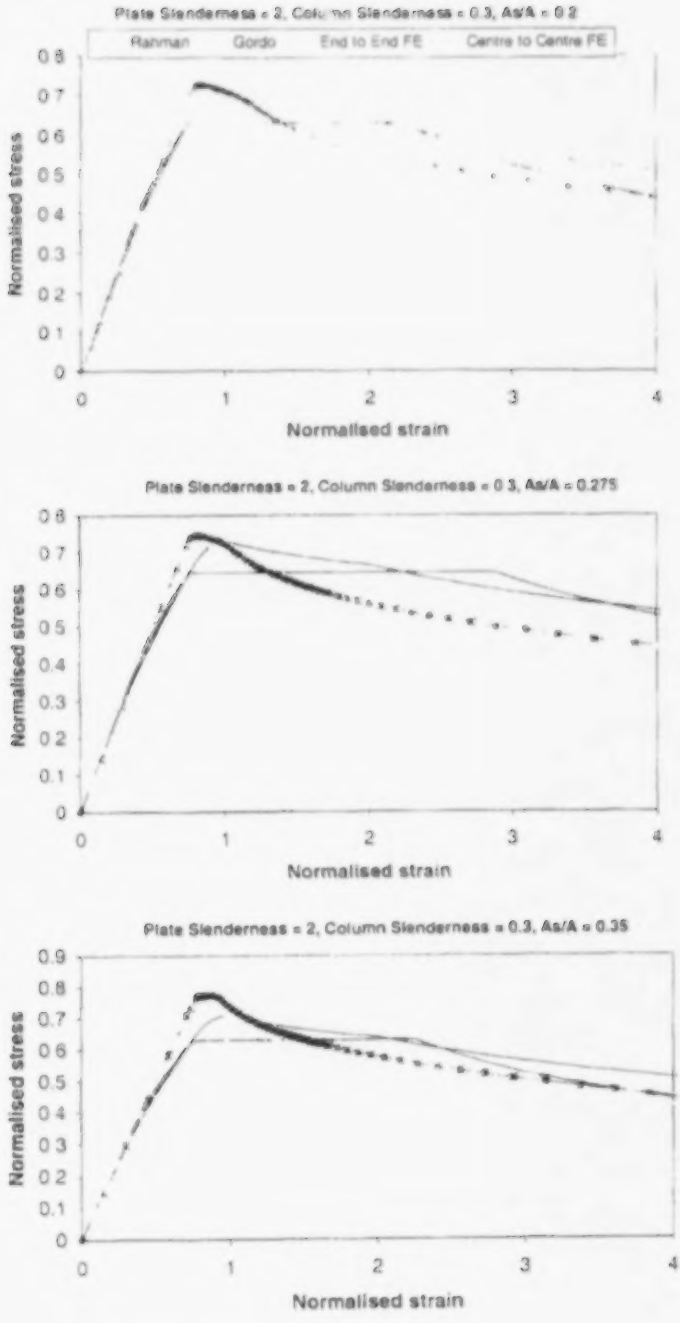
Plate Slenderness = 2, Column Slenderness = 0.3, As/A = 0.2
Rahman
Gordo
End to End FE
Centre to Centre FE
Normalised stress
Normalised strain
Plate Slenderness = 2, Column Slenderness = 0.3, As/A = 0.275
Normalised stress
Normalised strain
Plate Slenderness = 2, Column Slenderness = 0.3, As/A = 0.35
Normalised stress
Normalised strain

Figure A.5: *Curves for* $\beta = 2$ *and* $\lambda = 0.3$.

P517010.PDF [Page: 66 of 91]

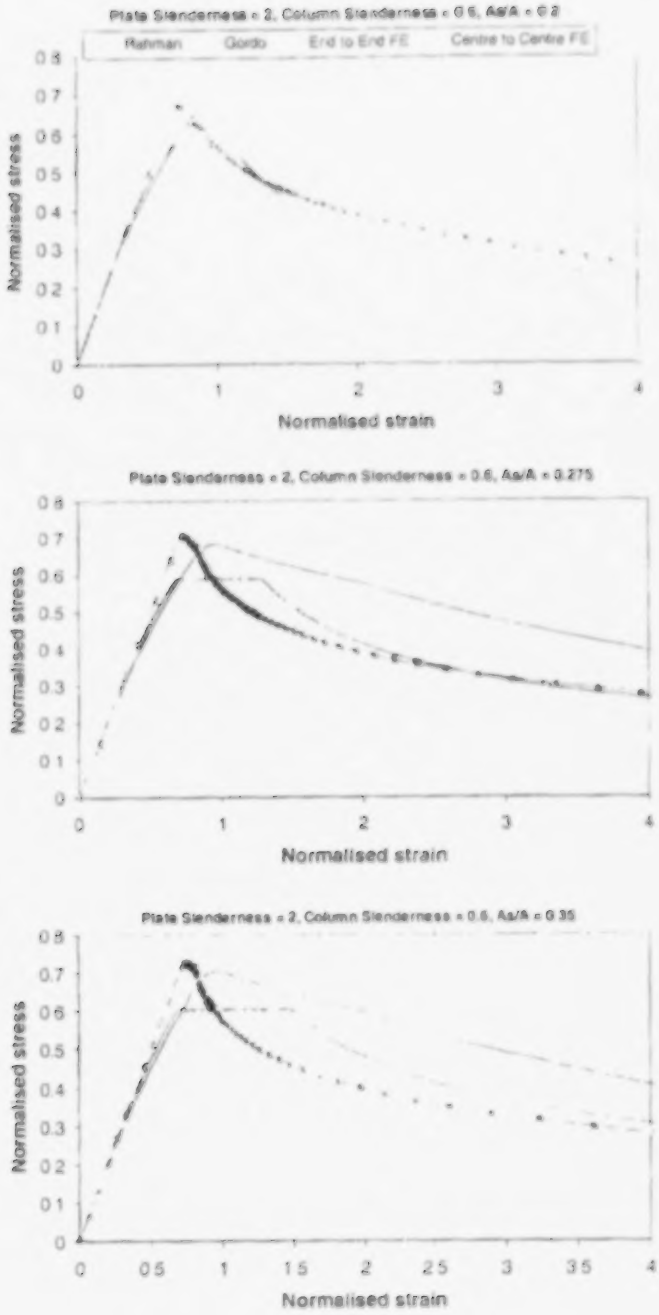
Plate Slenderness = 2, Column Slenderness = 0.6, As/A = 0.2
Rahman
Gordo
End to End FE
Centre to Centre FE
Normalised stress
Normalised strain
Plate Slenderness = 2, Column Slenderness = 0.6, As/A = 0.275
Normalised stress
Normalised strain
Plate Slenderness = 2, Column Slenderness = 0.6, As/A = 0.35
Normalised stress
Normalised strain

Figure A.5: *Curves for* $\beta = 2$ *and* $\lambda = 0.6$.

P517010.PDF [Page: 67 of 91]

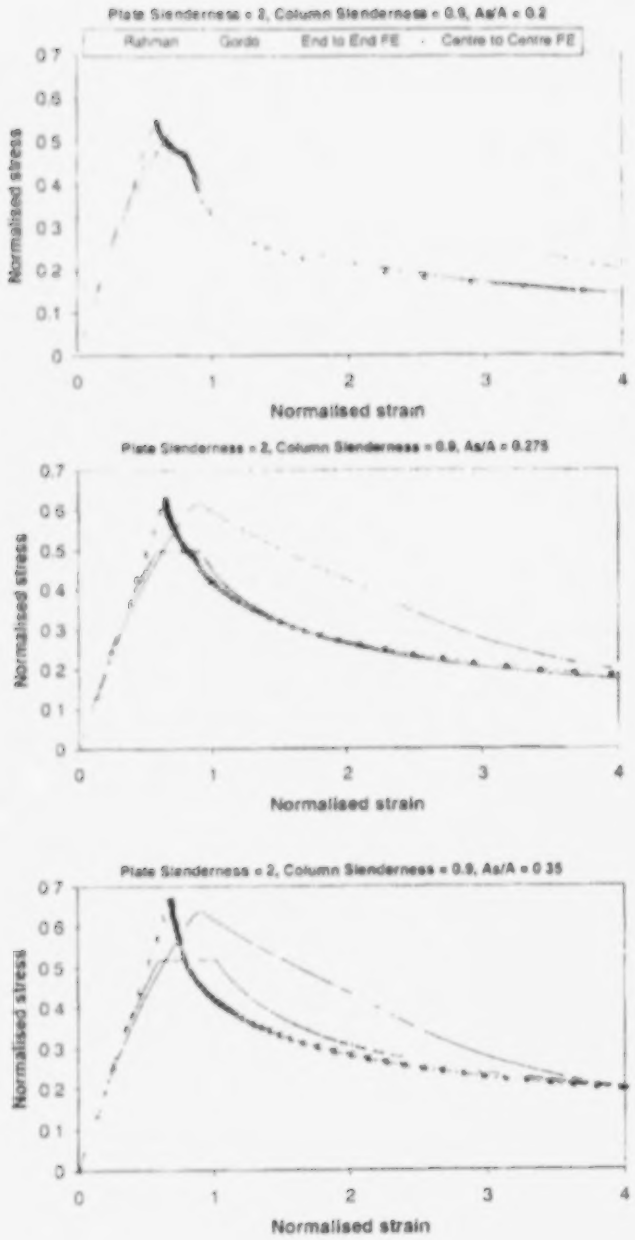
Plate Slenderness = 2, Column Slenderness = 0.9, As/A = 0.2
Rahman
Gordo
End to End FE
Centre to Centre FE
Normalised stress
Normalised strain
Plate Slenderness = 2, Column Slenderness = 0.9, As/A = 0.275
Normalised stress
Normalised strain
Plate Slenderness = 2, Column Slenderness = 0.9, As/A = 0.35
Normalised stress
Normalised strain

Figure A.7: *Curves for* $\beta = 2$ *and* $\lambda = 0.9$.

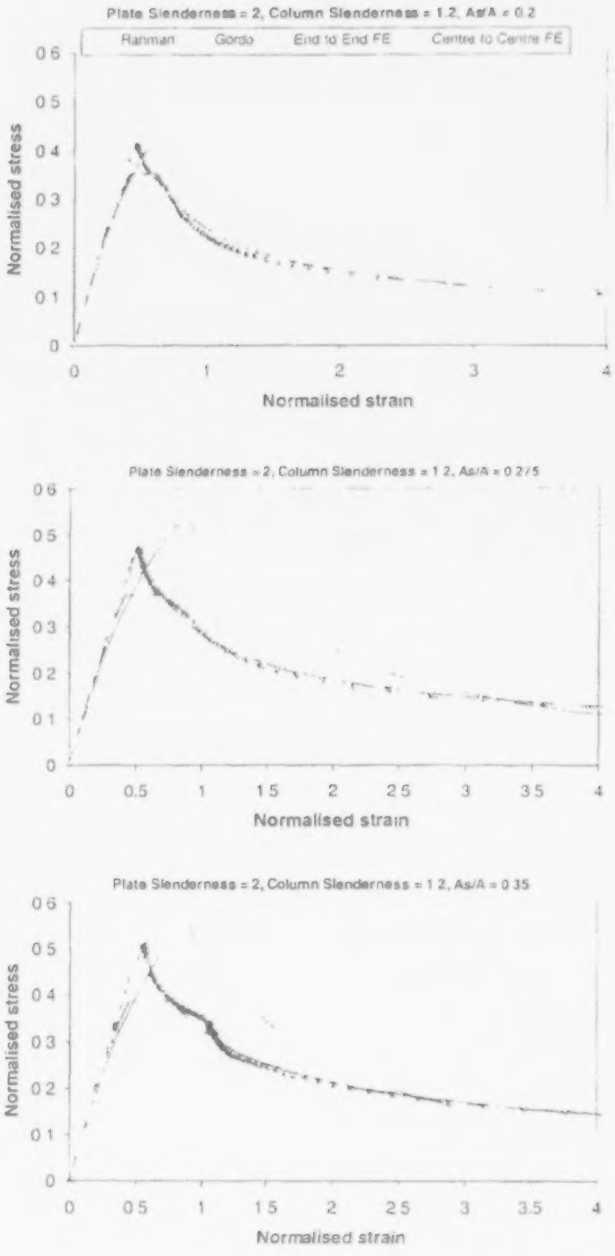
Plate Slenderness = 2, Column Slenderness = 1.2, As/A = 0.2
Rahman
Gordo
End to End FE
Centre to Centre FE
Normalised stress
Normalised strain
Plate Slenderness = 2, Column Slenderness = 1.2, As/A = 0.275
Normalised stress
Normalised strain
Plate Slenderness = 2, Column Slenderness = 1.2, As/A = 0.35
Normalised stress
Normalised strain

Figure A.8: *Curves for* $\beta = 2$ *and* $\lambda = 1.2$.

P517010.PDF [Page: 69 of 91]

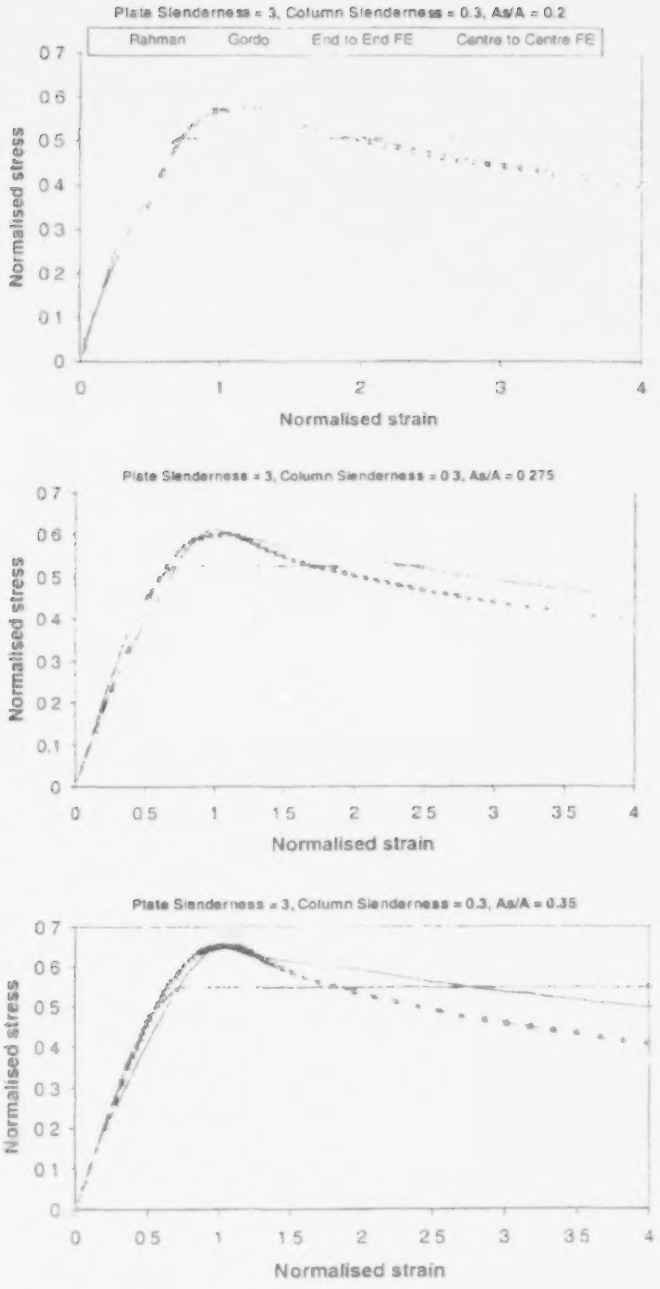
Plate Slenderness = 3, Column Slenderness = 0.3, As/A = 0.2
Rahman
Gordo
End to End FE
Centre to Centre FE
Normalised stress
Normalised strain
Plate Slenderness = 3, Column Slenderness = 0.3, As/A = 0.275
Normalised stress
Normalised strain
Plate Slenderness = 3, Column Slenderness = 0.3, As/A = 0.35
Normalised stress
Normalised strain

Figure A.9: *Curves for $\beta = 3$ and $\lambda = 0.3$.*

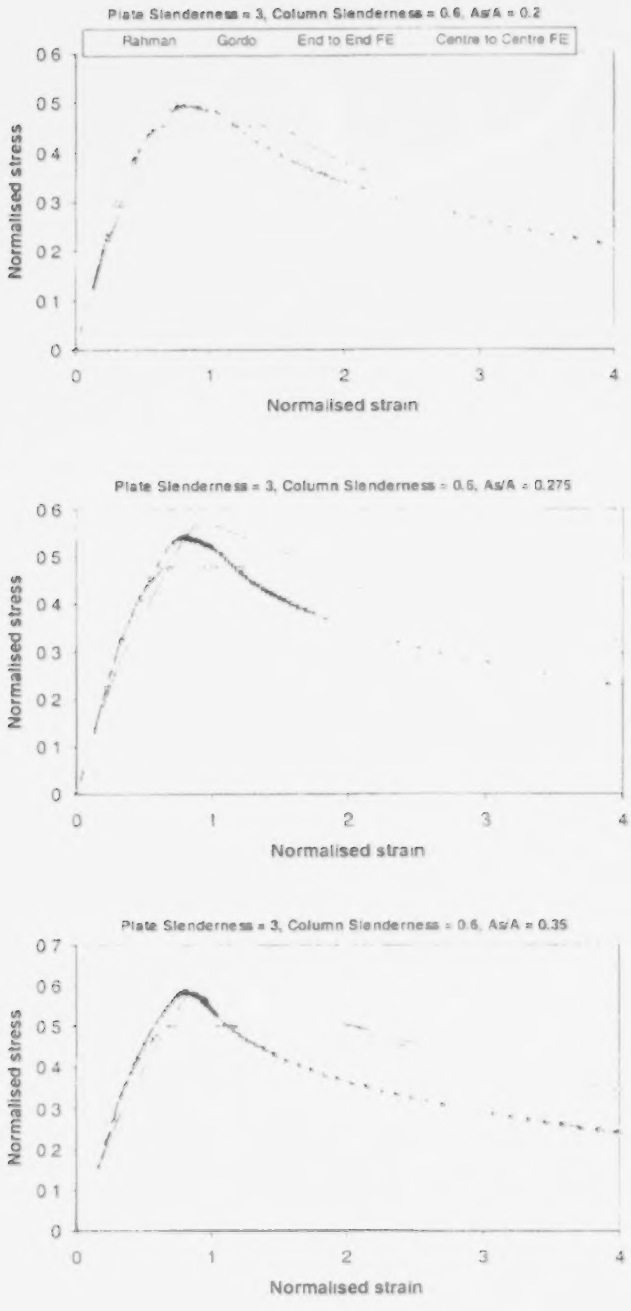
Plate Slenderness = 3, Column Slenderness = 0.6, As/A = 0.2
Rahman
Gordo
End to End FE
Centre to Centre FE
Normalised stress
Normalised strain
Plate Slenderness = 3, Column Slenderness = 0.6, As/A = 0.275
Normalised stress
Normalised strain
Plate Slenderness = 3, Column Slenderness = 0.6, As/A = 0.35
Normalised stress
Normalised strain

Figure A.10: *Curves for* $\beta = 3$ *and* $\lambda = 0.6$.

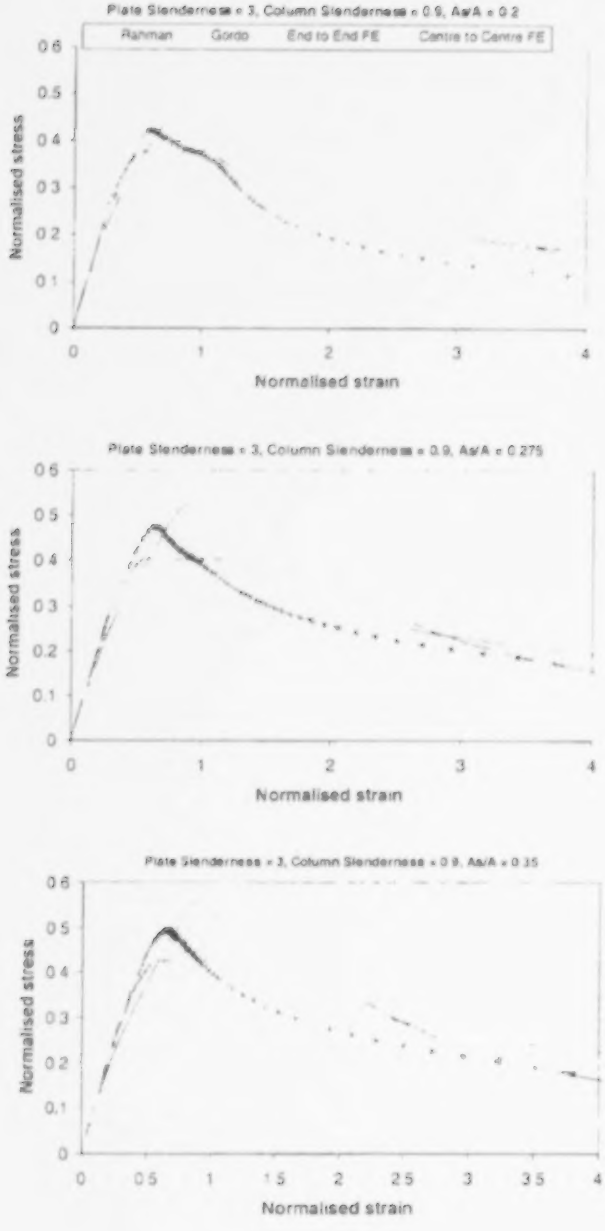
Plate Slenderness = 3, Column Slenderness = 0.9, As/A = 0.2
Rahman
Gordo
End to End FE
Centre to Centre FE
Normalised stress
Normalised strain
Plate Slenderness = 3, Column Slenderness = 0.9, As/A = 0.275
Normalised stress
Normalised strain
Plate Slenderness = 3, Column Slenderness = 0.9, As/A = 0.35
Normalised stress
Normalised strain

Figure A.11: *Curves for $\beta = 3$ and $\lambda = 0.9$.*

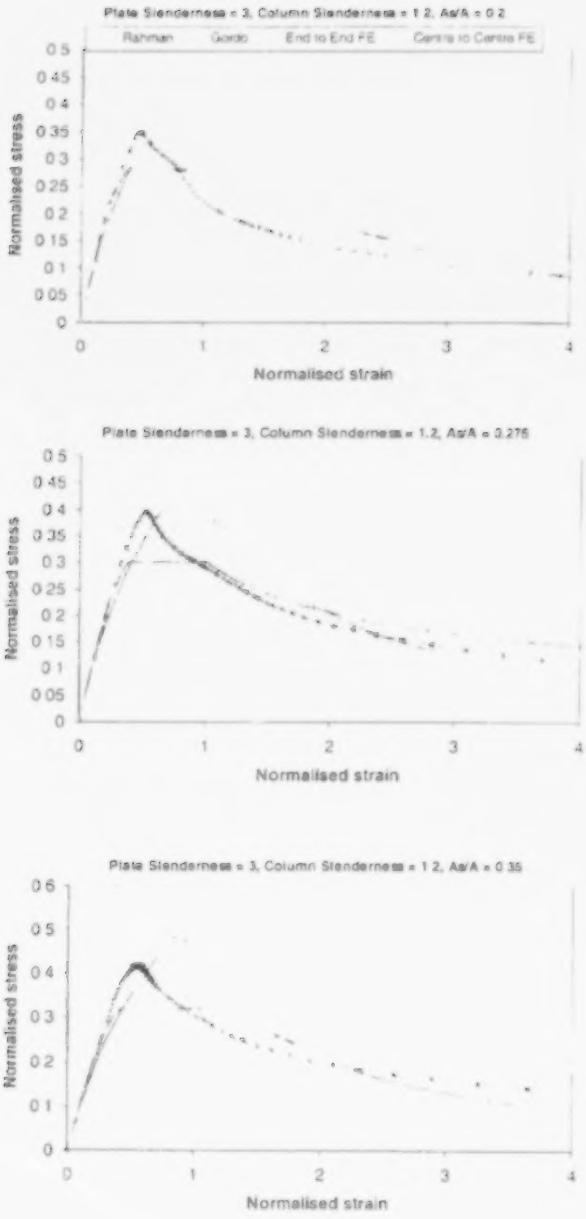
Plate Slenderness = 3, Column Slenderness = 1.2, As/A = 0.2
Rahman
Gerdo
End to End FE
Centre to Centre FE
Normalised stress
Normalised strain
Plate Slenderness = 3, Column Slenderness = 1.2, As/A = 0.275
Normalised stress
Normalised strain
Plate Slenderness = 3, Column Slenderness = 1.2, As/A = 0.35
Normalised stress
Normalised strain

Figure A.12: *Curves for* $\beta = 3$ *and* $\lambda = 1.2$.

P517010.PDF [Page: 73 of 91]

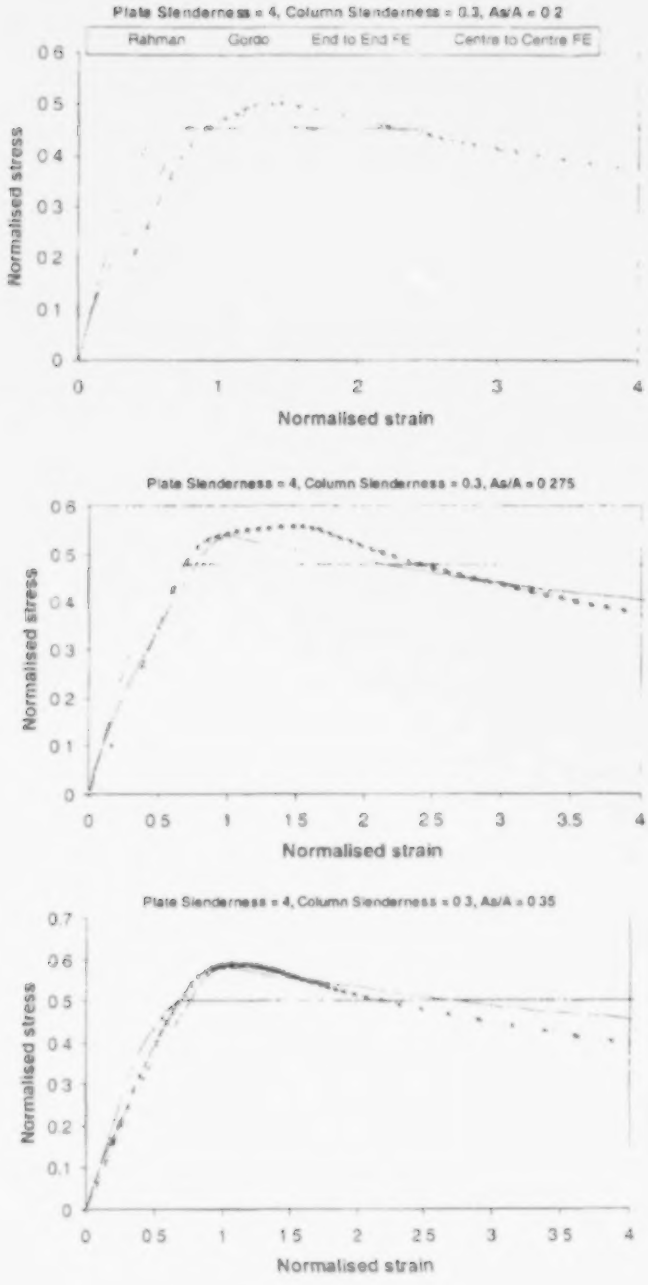
Plate Slenderness = 4, Column Slenderness = 0.3, As/A = 0.2
Rahman
Gordo
End to End FE
Centre to Centre FE
Normalised stress
Normalised strain
Plate Slenderness = 4, Column Slenderness = 0.3, As/A = 0.275
Normalised stress
Normalised strain
Plate Slenderness = 4, Column Slenderness = 0.3, As/A = 0.35
Normalised stress
Normalised strain

Figure A.13: *Curves for* $\beta = 4$ *and* $\lambda = 0.3$.

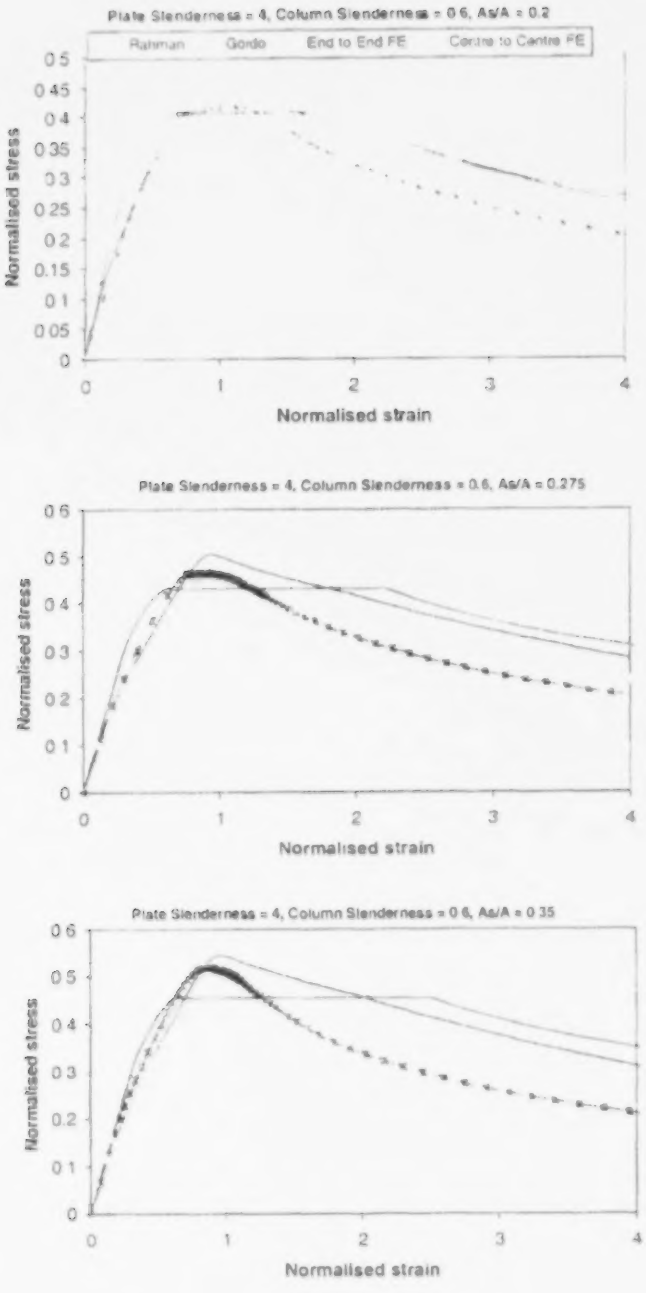
Plate Slenderness = 4, Column Slenderness = 0.6, As/A = 0.2
Rahman
Gordo
End to End FE
Centre to Centre FE
Normalised stress
Normalised strain
Plate Slenderness = 4, Column Slenderness = 0.6, As/A = 0.275
Normalised stress
Normalised strain
Plate Slenderness = 4, Column Slenderness = 0.6, As/A = 0.35
Normalised stress
Normalised strain

Figure A.14: *Curves for* $\beta = 4$ *and* $\lambda = 0.6$.

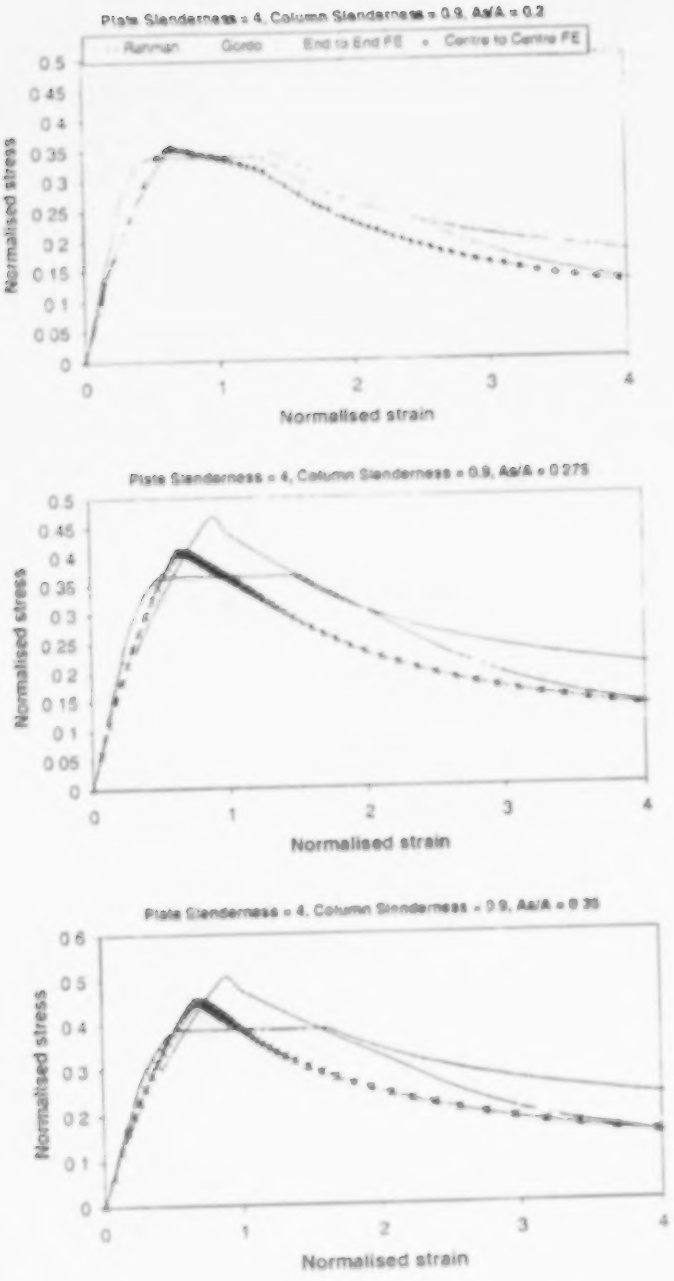
Plate Slenderness = 4, Column Slenderness = 0.9, As/A = 0.2
Rahman
Gordo
End to End FE
Centre to Centre FE
Normalised stress
Normalised strain
Plate Slenderness = 4, Column Slenderness = 0.9, As/A = 0.275
Normalised stress
Normalised strain
Plate Slenderness = 4, Column Slenderness = 0.9, As/A = 0.35
Normalised stress
Normalised strain

Figure A.15: Curves for $\beta = 4$ and $\lambda = 0.9$.

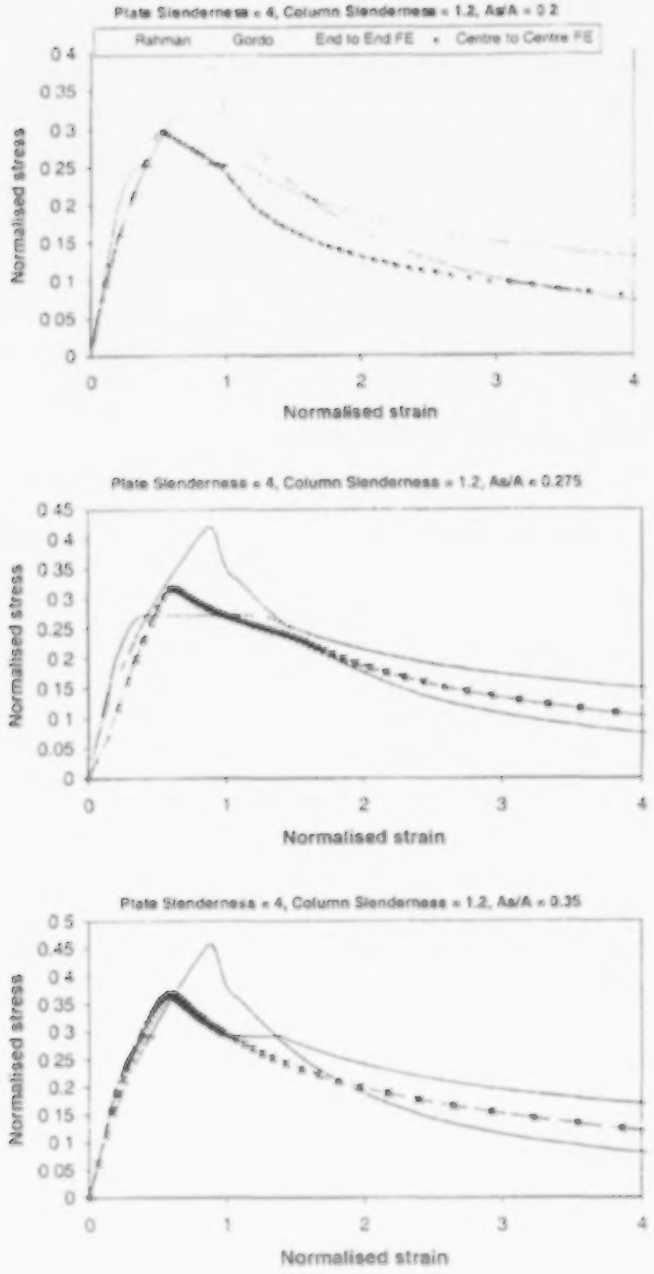
Plate Slenderness = 4, Column Slenderness = 1.2, As/A = 0.2
Rahman
Gordo
End to End FE
Centre to Centre FE
Normalised stress
Normalised strain
Plate Slenderness = 4, Column Slenderness = 1.2, As/A = 0.275
Normalised stress
Normalised strain
Plate Slenderness = 4, Column Slenderness = 1.2, As/A = 0.35
Normalised stress
Normalised strain

Figure A.16: *Curves for* $\beta = 4$ *and* $\lambda = 1.2$.

Annex B
User's Guide to RESULTS 1.0

B.1 Master data file

The master data file *jobname*.usx contains information specifying the type of ultimate strength analysis to be performed, as well as the names, locations and formats of the input and output data files. A *jobname*.usx file must be provided for every RESULTS analysis. Formatting of the *jobname*.usx file is described in the sections listed below.

B.1.1 Defining the analysis type

The type of ultimate strength analysis is defined by an `Execute` statement. The form of the `Execute` statement to be used depends on the type of analysis type to be performed. The various forms are described below.

B.1.1.1 Bi-axial moment-curvature analysis

This performs a moment-curvature analysis in a user-defined direction.

```
Execute BiaxialMC {
    Direction dirAngle
    StepSize  curvatureStepSize
    Steps     numSteps
}
```

where

- *dirAngle* is the angle of the neutral axis of bending, measured counter-clockwise from the positive lateral axis (float).
- *curvatureStepSize* is the scalar step size used to increment the applied curvature (float)
- *numSteps* is the number of curvature steps to be taken (int)

B.1.1.2 Hog and sag moment-curvature analysis

This performs the two vertical bending moment-curvature analyses

```
Execute HogAndSagMC {
    StepSize curvatureStepSize
    Steps    numSteps
}
```

where

- *curvatureStepSize* the scalar curvature increment size, expressed as a fraction of the first-yield hull curvature in the defined direction (float)
- *numSteps* is the number of curvature steps to be taken (int)

B.1.1.3 Bi-axial static strength analysis

This finds the maximum bending moment in a user-defined direction.

```
Execute BiaxialStrength {
    Direction dirAngle
    StepSize  momentStepSize
}
```

where

- *dirAngle* is the angle of the neutral axis of bending, measured counter-clockwise from the positive lateral axis (float)
- *momentStepSize* is the scalar moment increment size, expressed as a fraction of the first-yield bending moment in the defined direction (float)

B.1.1.4 Interaction curve analysis

This performs a series bi-axial strength analyses in different directions to produce an envelope of maximum bending moments

P517010.PDF [Page 79 of 91]

```
Execute InteractionCurve {
    StepSize momentStepSize
    Points   numPoints
}
```

where

- *numPoints* is the number of equally spaced points in the interaction curve
- *momentStepSize* is the scalar moment increment size used to calculate all points. The step size is expressed as a fraction of the first-yield bending moment in the defined direction (float)

B.1.1.5 First-yield bending moment analysis

This finds the bending moment that produces a first-yield condition in a structural unit, ignoring the buckling behaviour of the structural units in compression.

```
Execute YieldMoment {
    Direction dirAngle
}
```

where *dirAngle* is the angle of the neutral axis of bending, measured counter-clockwise from the positive lateral axis (float).

B.1.1.6 Plastic bending moment analysis

This finds the fully-developed plastic bending moment in a user-defined direction.

```
Execute PlasticMoment {
    Direction dirAngle
}
```

where *dirAngle* is the angle of the neutral axis of bending, measured counter-clockwise from the positive lateral axis (float).

B.1.2 Cross section data file

The cross-section data file is defined using the `XSectionData` command.

```
XSectionData {
    format formatType
    file   fileName
}
```

where

- *formatType* is a string identifier defining the cross-section format. Allowable types are generic and ultmat (string).
- *fileName* is the name of the file (including path) containing the cross section data (string).

Additional information on cross section definition can be found in Annex B.2.

B.1.3 Materials data file

The materials data file is defined using the `MaterialsData` command.

`MaterialsData` *fileName*

where *fileName* is the name of the file (including path) containing the materials data (string).

Additional information on materials definition can be found in Annex B.3.

B.1.4 Load shortening curve databases

Load shortening curve databases and data files are specified with the `LSCurveData` command.

```
LSCurveData {
    dataBase dataBaseName
    file     fileName
}
```

where

- *dataBaseName* is the name of the L-S curve database to be used for interpolating stress-strain behaviour (string). Three L-S curve databases are available to the user: `NS94`, `EndToEndCPF`, and `CentreToCentreCPF`
- *fileName* is the name of the file (including path) containing the specific L-S curves (string).

Additional data on defining specific L-S curves can be found in Annex B.4.

B.1.5 Results and other output files

The file containing the results of the ultimate strength analysis is specified with the `ResultsFile` command.

`ResultsFile` *`fileName`*

where *`fileName`* is the name of the file (including path) where the analysis results are to be written (string).

In addition to the results file, the programme will also create a file *jobname*.err that contains error or warning messages pertaining to the analysis.

B.2 Cross section data formats

The cross-sectional model for a RESULTS is defined in terms of its longitudinal structural units. Structural units can be longitudinal or transversely stiffened panels, or hard corners.

Two data formats can be used to define the cross sectional model:

- ULTMAT format
- Generic format

B.2.1 ULTMAT format

This format is the same as the one generated by ULTSAS for use the the old ULTMAT code. The first two lines of data are:

`title`
`numUnits E`

where

- *`title`* is a literal string constant
- *`numUnits`* is the number of structural units in the model (int).
- *`E`* is the elastic modulus of the model material (float).

The following *`numUnits`* lines have the format:

P517010.PDF [Page: 82 of 91]

```
index A y z lambda beta sigma
```

where

- *index* is an integer identifier for the ith unit (float).
- *A* is the cross-sectional area of the ith unit (float).
- *y* is the vertical position of the ith unit's centroid (float).
- *z* is the lateral position of the ith unit's centroid (float).
- *lambda* is the column slenderness of the ith unit (float).
- *beta* is the plate slenderness of the ith unit (float).
- *sigma* is the yield stress of the ith unit (float).

B.2.2 Generic format

The first line of the file must have the statement:

```
#Units numUnits
```

where *numUnits* is the number of structural units in the model.

The remainder of the file lists the definitions of the individual units in any order. A structural unit is defined with a statement of the following generalised form:

```
UnitTypeName {
    material matName
    position yPos zPos
    area     xSectionArea
    LSCurve  curveName
    ...  etc.
}
```

where

- *UnitTypeName* identifies the type of structural unit (string). Three types may be defined.
  - *UnitTypeName* = LongStiffPanel for longitudinally stiffened panels.

P517010.PDF [Page: 83 of 91]

- *UnitTypeName* = TranStiffPanel for transversely stiffened panels.
- *UnitTypeName* = HardCorner for hard corner units.

- *matName* is the name of the unit material (string).
- *yPos* is the horizontal position of the unit centroid (float).
- *zPos* is the vertical position of the unit centroid (float).
- *xSectionArea* is the cross sectional area of the unit (float).
- *curveName* is the name of a specific load-shortening curve to be with this panel (string). This LSCurve statement is optional. If it is omitted, the load-shortening properties of the unit will be interpolated from the database.

All the structural unit types require material, position, and area statements. Additional statements needed to define the structural units is given below.

B.2.2.1 Longitudinally stiffened panels

Four additional statements are needed for this type of unit.

```
columnSlender lambdaValue
plateSlender  betaValue
areaRatio     arValue
imperfection  imperfLevel
```

where

- *lambdaValue* is the column slenderness value (λ) for the panel (float).
- *betaValue* is the plate slenderness (β) for the panel (float).
- *arValue* is the stiffener-area to total-area ratio (A_s/A) for the panel (float).
- *imperfLevel* is a string identifier defining the level of imperfection (geometric and residual stresses) in the panel (string). Allowable strings are SLIGHT, AVERAGE and SEVERE.

P517010.PDF [Page: 84 of 91]

B.2.2.2 Transversely stiffened panels

Four additional statements are needed for this type of unit.

```
plateSlender betaValue
aspectRatio  alphaValue
```

where

- `betaValue` is the plate slenderness (β) for the panel (float).
- `alphaValue` is the panel aspect ratio (a/b) (float).

B.2.2.3 Hard corner units

No additional information is needed for these units.

B.3 Materials file format

The material properties of the structural units have to be defined in a separate file only when the generic cross section data format is used.

The file lists the definitions of the individual materials in any order. A material is defined with a statement of the following form:

```
Material {
    modulus     E
    yieldStress sigmaY
    yieldStrain epsilonY
}
```

where

- `E` is the elastic modulus of the material (float).
- `sigmaY` is the yield stress value (float).
- `epsilonY` is the yield strain (float).

The modulus statement must be supplied for all materials. At least one of either the `yieldStress` or the `yieldStrain` statements must also be provided.

P517010.PDF [Page: 85 of 91]

B.4 Defining additional load shortening curves

If load-shortening curves in addition to those in the databases are to be used in an analysis, they must be included in a separate file. The name of the file is defined in `LSCurveData` command issued in the *jobname*.usx file.

Load shortening curves are identified by a unique character-string name provided with them. They can be listed in the file in any order.

A load-shortening curve is defined by a LSCurve statement:

```
LSCurve {
    name identifier
    curve {
        strain_i stress_i
        ...
    }
}
```

where *identifier* is the unique label for the curve (string).

The line

strain_i stress_i

denotes the vertices of a point in the curve, where

- *strain_i* is the strain (normalized to the yield strain) of a point in the curve (float).
- *stress_i* is the stress (normalized to yield stress) of a point in the curve (float).

A pair of strain, stress values is to be provided for each point in the curve (minimum of 2) inside the braces following the curve keyword.

B.5 Running RESULTS

Once the input data and *jobname*.usx have been created, the final step is to enter the jobname (path included) in the first line of a file called ResUltS.inp, located in the default execution directory. The programme can then be executed.

P517010.PDF [Page: 86 of 91]

List of symbols, abbreviations, acronyms and initialisms

Symbols

a	longitudinal length of a structural unit
A	cross-sectional area of a structural unit
A_e	effective cross-sectional area of a structural unit
A_r	reduced cross-sectional area
A_s	cross-sectional area of a longitudinal stiffener
b	plate width of a stiffened panel unit
b_e	effective plate width of a stiffened panel unit
b'_e	reduced effective plate width of a stiffened panel unit
b_{er}	effective plate width including residual stresses
D, D'	matrix of cross-sectional flexural rigidities
D_{hh}	lateral flexural rigidity of a cross section
D_{vv}	vertical flexural rigidity of a cross section
D_{hv}	cross-sectional coupling rigidity
E	material elastic modulus
E_s	material tangent modulus
I'_e	effective second moment of area of a stiffened panel in lateral bending
M	bi-axial bending moment vector
M_h	lateral component of bi-axial bending moment
M_p	plastic moment of a stiffened panel section
M_v	vertical component of bi-axial bending moment
ΔM	incremental moment vector
ΔM_h	incremental lateral bending moment
ΔM_v	incremental vertical bending moment
ΔM_{err}	incremental error moment vector
$\Delta M'$	adjusted incremental moment vector
P	axial load
P_{ult}	axial load
q	lateral load per unit length on a stiffened panel
r	radius of gyration of a stiffened panel in lateral bending
t	plate thickness
T	ratio of tangent modulus to elastic modulus ($= E_s/E$)
T_r	reduced plate thickness
w_{max}	lateral deflection of a stiffened panel when a plastic hinge is fully formed
w_T	lateral deflection of a stiffened panel after a plastic hinge is formed
w_{ult}	lateral deflection of a stiffened panel when carrying its maximum load
y_i	vertical position of a structural unit

P517010.PDF [Page: 87 of 91]

z_t	lateral position of a structural unit
$\overline{y}$	vertical position of the cross-sectional centroid
$\overline{z}$	lateral position of the cross-sectional centroid
α	aspect ratio of structural unit $= a/b$
β	plate slenderness parameter (based on yield stress)
β_e	plate slenderness parameter (based on edge stress)
δ_p	maximum plate imperfection
δ_s	maximum stiffener imperfection
ϵ	longitudinal strain
ϵ_{pl}	longitudinal strain at which a stiffened panel's plastic hinge is fully formed
ϵ_{ult}	longitudinal strain at which a stiffened panel's ultimate strength is reached
ϵ_y	material yield strain
$\overline{\epsilon}$	normalised longitudinal strain $(= \epsilon/\epsilon_y)$
η	structural unit strength reduction factor
κ, κ'	bi-axial curvature vector
κ_h	lateral component of curvature
κ_v	vertical component of curvature
$\Delta\kappa$	incremental curvature vector
$\Delta\kappa_h$	incremental lateral curvature
$\Delta\kappa_v$	incremental vertical curvature
κ_{max}	maximum allowable curvature
λ	column slenderness parameter
ξ	parameter used to define the material tangent modulus
σ	longitudinal stress
σ_a	average longitudinal stress
σ_e	edge longitudinal stress
σ_r	compressive residual stress in plating
σ_y	material yield stress
$\overline{\sigma}$	normalised longitudinal stress $(= \sigma/\sigma_y)$
$\overline{\sigma}_a$	normalised average longitudinal stress $(= \sigma_a/\sigma_y)$
$\overline{\sigma}_r$	normalised residual stress $(= \sigma_r/\sigma_y)$
$\overline{\sigma}_{ult}$	normalised stiffened panel ultimate strength
$\overline{\sigma}_{uf}$	normalised ultimate strength for stiffener flange failure
$\overline{\sigma}_{up}$	normalised ultimate strength for plating flange failure
ϕ	angular position of cross-sectional loading axis
Φ_e	elastic/perfectly-plastic material strength parameter
Φ_E	Euler elastic column strength parameter
Φ_{jo}	Johnson-Ostenfeld column strength parameter
Φ_r	elastic/perfectly-plastic strength parameter including residual stresses
Φ_R	effective plate width reduction parameter

P517010.PDF [Page: 88 of 91]

Acronyms

CF	Canadian Forces
CPF	Canadian Patrol Frigate
DND	Department of National Defence
DRDC	Defence Research and Development Canada
FABSTRAN	Frame and Beam Static and Transient Response Analysis
FE	finite element
FEA	finite element analysis
ISSMM	Improved Ship Structure Maintenance Management
IST	ISSMM Software Tool
L-S	load-shortening
LSC	load-shortening curve
MOD	Ministry of Defence (UK)
PCM	Progressive Collapse Method
RESULTS	Residual and Ultimate Strength
ULTSAS	Ultimate Strength Analysis Suite
ULTSTR	US Navy ultimate strength analysis programme
VAST	Vibration and Strength Analysis

P517010.PDF [Page: 89 of 91]

UNCLASSIFIED
SECURITY CLASSIFICATION OF FORM
(highest classification of Title, Abstract, Keywords)

DOCUMENT CONTROL DATA

(Security classification of title, body of abstract and indexing annotation must be entered when the overall document is classified)

1 ORIGINATOR (the name and address of the organization preparing the document. Organizations for whom the document was prepared, e.g. Establishment sponsoring a contractor's report, or tasking agency, are entered in section 8.)

Defence Research Establishment Atlantic
PO Box 1012
Dartmouth, Nova Scotia, Canada B2Y 3Z7

2. SECURITY CLASSIFICATION (overall security classification of the document including special warning terms if applicable)

UNCLASSIFIED

3 TITLE (the complete document title as indicated on the title page. Its classification should be indicated by the appropriate abbreviation (S,C,R or U) in parentheses after the title)

Progressive Collapse Method for Ultimate Hull Girder Strength Assessment

4 AUTHORS (Last name, first name, middle initial. If military, show rank, e.g. Doe, Maj. John E.)

Smith, Malcolm J.

5 DATE OF PUBLICATION (month and year of publication of document)	6a. NO. OF PAGES (total containing information. Include Annexes, Appendices, etc)	6b. NO. OF REFS (total cited in document)
October 2001	88	40

7 DESCRIPTIVE NOTES (the category of the document, e.g. technical report, technical note or memorandum. If appropriate, enter the type of report, e.g. interim, progress, summary, annual or final. Give the inclusive dates when a specific reporting period is covered)

TECHNICAL MEMORANDUM

8 SPONSORING ACTIVITY (the name of the department project office or laboratory sponsoring the research and development. Include address)

Defence Research Establishment Atlantic

9a. PROJECT OR GRANT NO. (if appropriate, the applicable research and development project or grant number under which the document was written. Please specify whether project or grant)	9b. CONTRACT NO. (if appropriate, the applicable number under which the document was written)
Project 1.g.c.14	

10a. ORIGINATOR'S DOCUMENT NUMBER (the official document number by which the document is identified by the originating activity. This number must be unique to this document.)	10b. OTHER DOCUMENT NOs. (Any other numbers which may be assigned this document either by the originator or by the sponsor.)
DREA TM 2001-145	

11 DOCUMENT AVAILABILITY (any limitations on further dissemination of the document, other than those imposed by security classification)

(x) Unlimited distribution
( ) Defence departments and defence contractors; further distribution only as approved
( ) Defence departments and Canadian defence contractors; further distribution only as approved
( ) Government departments and agencies; further distribution only as approved
( ) Defence departments; further distribution only as approved
( ) Other (please specify):

12 DOCUMENT ANNOUNCEMENT (any limitation to the bibliographic announcement of this document. This will normally correspond to the Document Availability (11). However, where further distribution (beyond the audience specified in (11) is possible, a wider announcement audience may be selected)

UNCLASSIFIED
SECURITY CLASSIFICATION OF FORM

P517010.PDF [Page: 90 of 91]

UNCLASSIFIED
SECURITY CLASSIFICATION OF FORM
(highest classification of Title, Abstract, Keywords)

13. ABSTRACT (a brief and factual summary of the document. It may also appear elsewhere in the body of the document itself. It is highly desirable that the abstract of classified documents be unclassified. Each paragraph of the abstract shall begin with an indication of the security classification of the information in the paragraph (unless the document itself is unclassified) represented as (S), (C), (R), or (U). It is not necessary to include here abstracts in both official languages unless the text is bilingual)

This Memorandum provides a description of the theory and use of the progressive collapse method (PCM) for deterministic evaluation of a ship's hull girder ultimate strength. Bi-axial ultimate strength is considered, in which bending of a ship can occur about any axis in a cross-sectional plane perpendicular to the longitudinal axis. Two algorithms are examined for determining the ultimate strength: moment-curvature analysis, in which curvature incrementing is used, and bi-axial strength analysis, in which moment incrementing is used. The merits of these two algorithms are considered for determining interaction curves defining the envelope of bi-axial ultimate strengths. The load-carrying characteristics of individual structural units are also examined, and a review of the theory and assumptions is given. Two approaches for generating load-shortening response curves of longitudinally stiffened panels are considered in detail: one involves interpolation from precalculated load-shortening curves and the other involves the use of design formulas. The implementation of the PCM in the RESULTS (RESidual and ULTimate Strength) programme is described, and a user's guide is provided. Validation of the code is performed using a steel box girder structure and two hypothetical damage case studies involving the HALIFAX class warship.

14. KEYWORDS, DESCRIPTORS or IDENTIFIERS (technically meaningful terms or short phrases that characterize a document and could be helpful in cataloguing the document. They should be selected so that no security classification is required. Identifiers, such as equipment model designation, trade name, military project code name, geographic location may also be included. If possible keywords should be selected from a published thesaurus, e.g. Thesaurus of Engineering and Scientific Terms (TEST) and that thesaurus identified. If it not possible to select indexing terms which are Unclassified, the classification of each should be indicated as with the title)

Ship structure
Ultimate strength
Hull girder
Progressive failure method
Load shortening curve
Stiffened panel
Moment curvature analysis
Bi-axial bending

UNCLASSIFIED
SECURITY CLASSIFICATION OF FORM

P517010.PDF [Page: 91 of 91]

Defence R&D Canada
is the national authority for providing
Science and Technology (S&T) leadership
in the advancement and maintenance
of Canada's defence capabilities.

R et D pour la défense Canada
est responsable, au niveau national, pour
les sciences et la technologie (S et T)
au service de l'avancement et du maintien des
capacités de défense du Canada.

#517010
CA020266

DEFENCE R&D DÉFENSE

www.drdc-rddc.dnd.ca